

**Effect of sodium chloride on the
formation of ice and salt during eutectic
freeze crystallization of sodium sulfate
with a scenario study of real brine**

Hao Wu



Effect of sodium chloride on the formation of ice and salt during eutectic freeze crystallization of sodium sulfate with a scenario study of real brine

By Hao Wu

Section of Sanitary Engineering, Faculty of Civil Engineering & Geosciences
Department of Biotechnology, Faculty of Applied Science

Submitted in partial fulfilment of the requirements for the degree of

Master of Science

in Civil Engineering, Track of Environmental Engineering

at the Delft University of Technology

July. 2020

Assessment Committee:

TU Delft Dr. Ir. Henri Spanjers

TU Delft Dr. Ir. Sirous Ebrahimi

TU Delft Prof. Dr. Ir. Mark van Loosdrecht

TU Delft Dr. Ir. SGJ Heijman

An electronic version of this thesis is available at <http://repository.tudelft.nl>

Preface

The journey at the Delft University of Technology ends up with this thesis. The first glimpse of this town was quiet and leisure. I was curious about the people and multicultural life here. But the intensive class followed by the endless deadline quickly altered my feeling. Two years could change people a lot. I have developed with unparalleled speed in my professional area, reinforced independent thinking, and cultivated several new hobbies. Now it is time to embrace tomorrow and take on new challenges.

I would like to express my sincere gratitude to my committee. My chair supervisor Dr. Ir. Henri Spanjers who introduced the Eutectic Freeze Crystallization technology to me. Your guidance to my thesis and attention to detail is appreciated. Prof. Dr. Ir. Mark van Loosdrecht who enlightened me to think from different aspects of my research and always welcomed me to discuss anything with him. My daily supervisor Dr. Ir. Sirous Ebrahimi who offered me the most patient instruction during the whole process of my thesis. Dr. Ir. Bas Heijman who provided valuable advice to my research topics. Many thanks to the lab technicians Zita Krogt and Dirk Geerts at Department of Biotechnology, Faculty Applied Science for their contributions to my experiment set-up.

Thanks also go to my most motivated classmates and friends, many of the times we worked together to tackle the problems and watching the sunset on the top floor of our faculty. You gave me countless encouragement and tolerated my occasional crossness. The positive attitude and energy we shared, the memory we gained together was the most valuable treasure in the past two years. We always said "Everything is going to be alright". It is the time to rise from the ashes. May we have a bright future.

Last but not least, I would like to express my deepest gratitude to my parents, who are my best solid backing. Without your love and support, I would not be able to make it this far. Thank you for giving me the chance to study abroad and supporting me to chase my dream. Every time when I doubted myself, lost direction, felt exhausted and depressed, you embrace me like a sound bay. Love you like I did yesterday and always forever.

Nothing is impossible to a willing heart.

Table of Contents

Preface	i
Table of Contents	ii
List of Tables	v
List of Figures	vi
Nomenclature	viii
Abstract	ix
Chapter 1 Introduction.....	1
1.1 Research background	1
1.2 Knowledge gaps and research objectives	2
1.2.1 Effect of NaCl on the recovery of Na ₂ SO ₄	2
1.2.2 Research questions and approaches	3
1.3 Thesis structure	3
Chapter 2 Theory and Literature Review.....	4
2.1 Mechanisms of crystallization	4
2.1.1 Phase diagram	4
2.1.2 Supersaturation	5
2.1.3 Crystallization.....	5
2.1.4 Crystal lattice	6
2.1.5 Nucleation of crystals	6
2.1.6 Crystal growth.....	6
2.1.7 Product characteristics.....	7
2.2 Fundamentals of EFC technology.....	7
2.3 Processing modes of EFC.....	8
2.4 Heat transfer in eutectic freeze crystallization.....	9
2.5 Recover Na ₂ SO ₄ by EFC	10
2.6 Impurity Studies in EFC.....	10
2.7 The mechanism of impurities incorporated into crystallization	11
2.8 Ice scaling in scraped wall crystallizer	12
Chapter 3 Experimental study on the effect of NaCl concentrations.....	13
3.1 Materials.....	13
3.2 Experimental design and reagents	14
3.3 Experimental procedure.....	14
3.4 Measurements	15
3.4.1 Temperature.....	15
3.4.2 Concentration.....	15
3.4.3 Stirring torque.....	15
Chapter 4 Modelling study about continuous EFC of Na₂SO₄.....	16

4.1	OLI Stream Analyser modelling procedure	16
4.2	Effect of NaCl concentration on the solubility of Na ₂ SO ₄	18
4.3	A scenario study: effect of pretreatment on the product yield and recovery in continuous EFC of Na ₂ SO ₄	18
4.3.1	Effects of different Na ₂ SO ₄ concentrations in EFC.....	19
4.3.2	Effect of NaCl concentrations on the recovery of Na ₂ SO ₄ and ice	19
4.3.3	Scenario 1:RO-NF-EFC	19
4.3.4	Scenario 2:RO-TOC-NF-EFC.....	20
4.3.5	Scenario 3:RO-TOC-EFC	20
4.3.6	Scenario 4:RO-TOC-NF-RO-EFC.....	20
Chapter 5 Results and discussions.....		22
5.1	Effect of high concentration NaCl on EFC of Na ₂ SO ₄ from the aspects of temperature and product composition	22
5.1.1	Na ₂ SO ₄ - H ₂ O binary phase diagram	22
5.1.2	Comparison of experimental phase equilibria with modelling results	25
5.1.3	Compare the effect of salt with common ion and uncommon ion on the solubility of Na ₂ SO ₄	26
5.2	Scenario Study of using EFC to treat RO retentate	28
5.2.1	Effect of different Na ₂ SO ₄ concentration in EFC	28
5.2.2	Effect of NaCl concentration on the recovery of Na ₂ SO ₄ and ice.....	29
5.2.3	Scenario 1: RO-NF-EFC	31
5.2.4	Scenario 2: RO-TOC-NF-EFC.....	35
5.2.5	Scenario 3: RO-TOC-EFC	36
5.2.6	Scenario 4: RO-TOC-NF-RO-EFC.....	37
Chapter 6 Conclusions		40
Chapter 7 Research limitations and recommendations.....		42
7.1	The experiment set up and design.....	42
7.2	Modelling study about continuous EFC.....	43
References		44
Appendix		47
	Appendix A: Experiment set-up.....	47
	Appendix B: Thermodynamic model input of OLI Analyser	48
	Appendix C: Fitting curves and K _{sp} values.....	53
	Appendix D: Experimental error of Na ₂ SO ₄ solubility at three NaCl concentrations.....	54
	Appendix E: Decreasing rate of the solubility of Na ₂ SO ₄ with temperature at different NaCl/KCl concentrations	55
	Appendix F: Decreasing and decreasing rate of the solubility of Na ₂ SO ₄ with temperature.....	56

Appendix G: Temperature profile of the EFC process 57

List of Tables

Table 4.1 Three models provided in OLI Stream Analyser	17
Table 5.1 Nucleation temperatures and solid recovery for solid compounds when NaCl concentration varies from 0~150 g/L.....	29
Table 5.2 Nucleation temperature of solid products in scenario 1	32
Table 5.3 Nucleation temperature of solid products in scenario 2	36
Table 5.4 Nucleation temperature of solid products in scenario 3	37
Table 5.5 Nucleation temperature of solid products in scenario 4	38
Table A1 Model input: effect of NaCl concentrations on the solubility of Na ₂ SO ₄	48
Table A2 Model input: effect of KCl concentrations on the solubility of Na ₂ SO ₄	48
Table A3 Model input: the ice yield at different Na ₂ SO ₄ concentrations.....	48
Table A4 Model input of the simulation about the effect of NaCl on the recovery of mirabilite	48
Table A5 Ion concentration of NF concentrate, scenario 1	49
Table A6 Ion concentration of NF concentrate after TOC removal unit, scenario 2	50
Table A7 Ion concentration in effluent of TOC removal unit, scenario 3	51
Table A8 Ion concentration in the last RO retentate, scenario 4	52
Table A9 Fitting functions, solubility calculation results, ion concentrations and K _{sp} of Na ₂ SO ₄ at 0°C when NaCl concentration changes	53
Table A10 Fitting functions, solubility calculation results, ion concentrations and K _{sp} of Na ₂ SO ₄ at 5°C when NaCl concentration changes	53
Table A11 Error calculation about three concentrations of NaCl under different temperature	54
Table A12 The decreasing tendency of the solubility of Na ₂ SO ₄ with temperature when NaCl concentration changed.....	55
Table A13 The decreasing tendency of the solubility of Na ₂ SO ₄ with temperature when KCl concentration changed	55

List of Figures

Figure 2.1 Binary phase diagram of element A and B. A mixture of A and B.....	5
Figure 2.2 phase equilibria in the ternary system ¹⁷	5
Figure 2.3 A point lattice ¹²	6
Figure 2.4 A, B, C, three sites molecules can incorporate into the crystal surface	7
Figure 2.5 A simplest water–salt phase diagram at constant pressure ²⁰	8
Figure 2.6 Schematic representation of continuous EFC process for the production of pure water and salt ⁴	9
Figure 3.1 Experimental set-up for solubility experiments	13
Figure 3.2 Experiment procedure to determine the salt line.....	14
Figure 3.3 Experiment procedure to determine the ice line	15
Figure 4.1 Thermodynamic modelling procedure in OLI Stream Analyser	17
Figure 4.2 Process diagram of scenario 1	20
Figure 4.3 Process diagram of scenario 2	20
Figure 4.4 Process diagram of scenario 3	20
Figure 4.5 Process diagram of scenario 4	21
Figure 5.1 Binary phase diagram of Na ₂ SO ₄ - H ₂ O system changes with NaCl concentrations determined by experiment	23
Figure 5.2 EP of Na ₂ SO ₄ - H ₂ O system and eutectic concentration of Na ₂ SO ₄ with different NaCl concentrations obtained by experiment.....	23
Figure 5.3 Binary phase diagram for Na ₂ SO ₄ -H ₂ O showing regions of stable phases ³⁰ ..	24
Figure 5.4 Theoretical binary phase diagram of Na ₂ SO ₄ - H ₂ O system changes with NaCl concentrations	26
Figure 5.5 The change of the Na ₂ SO ₄ - H ₂ O system EP and eutectic concentration with different addition of NaCl (0-200 g/L).....	26
Figure 5.6 Theoretical binary phase diagram of Na ₂ SO ₄ - H ₂ O changes with KCl concentrations	27
Figure 5.7 EP of Na ₂ SO ₄ – H ₂ O system and eutectic concentration of Na ₂ SO ₄ with different addition of KCl (0-150 g/L)	28
Figure 5.8 Effect of Na ₂ SO ₄ concentration on ice recovery	29
Figure 5.9 Solid yield at different NaCl concentrations in continuous EFC of Na ₂ SO ₄	30
Figure 5.10 Ice and Na ₂ SO ₄ recovery in the cooling process at different concentrations of NaCl	31
Figure 5.11 Product yields with temperature in scenario 1.....	32
Figure 5.12 Nucleation temperature of ice and Na ₂ SO ₄ at different number of concentrate times	33
Figure 5.13 Solid content and total mass at different number of stage at -3 °C in 1L of feed	34

Figure 5.14 Solid composition and total mass at different number of stage at -5°C in 1L of feed	34
Figure 5.15 Product yields with temperature in scenario 2.....	36
Figure 5.16 Product yields with temperature in scenario 3.....	37
Figure 5.17 Product yields with temperature in scenario 4.....	39
Figure A1 Crystallizer for the batch experiment	47
Figure A2 Consort C3010 multi-parameter analyser	47
Figure A3 Lauda RP4080 CW thermal controller	47
Figure A4 The decreasing and decreasing rate of Na ₂ SO ₄ solubility with temperature at different NaCl(left) or KCl(right) concentrations	56
Figure A5 Temperature and conductivity profile during EFC.....	57
Figure A6 Ice and mirabilite yield during the cooling process under the different NaCl concentrations.....	57

Nomenclature

CSD	Crystal size distribution
DWP	Drinking water plant
EFC	Eutectic freeze crystallization
EP	Eutectic point
FP	Freezing point
IC	Ion chromatography
IEX	Ion exchange
NF	Nanofiltration
RC	Reaction crystallization
RO	Reverse osmosis
SCWC	Scraped cooled wall crystallizer
SI	Saturation index
ZLD	Zero liquid discharge

Abstract

Brine streams from industry is a burden to the environment if not disposed properly. "Zero liquid discharge" (ZLD) is an ideal way of converting saline streams from waste to resource through multiple membrane-based or thermal-based treatment technologies. The utilization of the recovered resource minimizes both costs and environmental impacts. Among the brine treatment technologies, the Eutectic Freeze Crystallization (EFC) is a promising thermal-based technology to obtain water and salt in high purity. EFC technology has higher energy benefit and simpler equipment than conventional evaporation technology. This technology is feasible for continuously recovering pure salt and ice in different stages, and separating them spontaneously.

In this study, batch EFC experiment was conducted to determine the solubility curve of Na_2SO_4 under the different concentrations of NaCl. The effect of NaCl on the solubility of Na_2SO_4 at the low-temperature interval was investigated. It was found that with the increasing concentration of NaCl, the common ion effect between Na_2SO_4 and NaCl reduced the solubility of Na_2SO_4 and depressed the eutectic point (EP) of Na_2SO_4 - H_2O system. The decreasing EP showed a linear trend. A thermodynamic model in OLI Studio was used to evaluate the solubility of Na_2SO_4 as well. The modelling result was compared with the experimental data. The experimental result about the EP of Na_2SO_4 - H_2O system has a better agreement to the theoretical value than the eutectic concentration of Na_2SO_4 . Besides, the effect of NaCl was compared with KCl in the OLI Studio, the salting- in effect of KCl promoted the solubility of Na_2SO_4 .

A scenario study was carried out to explore a proper process to treat reverse osmosis (RO) concentrate from a demineralised-water-producing (DWP) plant that was rich in Na^+ , SO_4^{2-} and Cl⁻. The thermodynamic model was used to simulate the continuous EFC process and investigate how the different pre-treatment processes affect the recovery of Na_2SO_4 . Four scenarios with different pre-treatment technologies were put forward based on the existing processing facilities: Scenario 1: RO – NF – EFC, Scenario 2: RO – TOC – NF – EFC, Scenario 3: RO – TOC – EFC, Scenario 4: RO – TOC – NF – RO – EFC.

All the scenarios could reach more than 92% recovery of H_2O . Among the four scenarios, Scenario 4 accomplished the highest recovery of Na_2SO_4 (98.4%) by -3°C . But the scaling tendency and poor permeate quality of the second RO unit made spontaneously. The gap between ice yield and $\text{Na}_2\text{SO}_4 \cdot 10\text{H}_2\text{O}$ (Mirabilite) yield was significant in all the scenarios. It was suggested only to recover H_2O rather than both H_2O and Na_2SO_4 , which can be achieved by means of Scenario 1 or 3. In Scenario 2, the close nucleation temperature of ice and mirabilite brought problem for separation work.

To conclude, EFC is a newly emerging technology that can achieve a sequential removal of minerals from brine and is sustainable. There are barriers to overcome in impurity studies and those problems deserve attention. Further developments should be stimulated on recovering H_2O and salt with an advance retrieving method, for example the design of multi-stage separation process, and the synergistic effect of different ion species and the combined effect of the organic compounds.

Chapter 1 Introduction

1.1 Research background

Water scarcity has been a long-term global issue. It was estimated that more than 50% of the countries on our planet might face severe water stress or water shortage by 2025. By then, 70% of the population could encounter this scarcity ¹. The rising water demand coupled with a deficit of water supply accelerate this problem. Among the water supply boost strategies, desalination receives the most attention. Along with the development of desalination, safe disposal of brine waste and innovative management and disposal strategy has been a particular concern, also a challenge.

“Zero liquid discharge (ZLD)” is a concept to maximize the recovery of freshwater and minimize waste in the wastewater treatment process. During the process, the industrial brine streams are converted into useful resources, the contaminants are reduced to solid substance, and the salt compounds are concentrated. An advanced circular economy can be achieved by recovering and reusing the collected minerals that are with high quality and sufficient purity from the brines. In the meantime, the industrial saline wastewater streams can also be eliminated.

A project was launched to achieve sustainable ZLD ². In the project, EFC is one of the selected technologies to obtain fresh water and solid products with high quality and good market value. A treatment process combined reverse osmosis (RO), nanofiltration (NF) and EFC aims to eliminate the brine effluent, recover high purity sulphate salts.

EFC is a novel technology that can be an alternative for evaporative crystallization. It is capable of selectively precipitating salts, and can be used to purify the concentrated brine. The technology is based on the theory that when the temperature of the solution achieves the EP, the solid phase and aqueous phase are separated due to density difference ^{3 4 5}.

With the development of over two decades, EFC has been proven to be used for the treatment of brine from desalination techniques such as multi-flush, spent regenerant of ion exchange (IEX) and concentrate of RO. One of the advantages is that EFC produces pure salt(s) and ice. Besides, F. Van der Ham et al. (1998) demonstrated that EFC required less energy and lower costs compared to conventional evaporative crystallization process ^{5 6}.

In the practical application, product quality and purity are all influenced by impurities. Despite the fact that diverse research investigated the influence of different impurities on EFC

process, none of the previous studies detailed explained to what extent the presence of other salts alters the product nucleation temperature and solubility. And how the pre-treatment process influences the product recovery, which can provide a better solution for the sequential removal of salts from brine.

In this study, the objective was to experimentally investigate the influence of concentrated NaCl on the EFC of Na₂SO₄ from the aspects of the eutectic concentration and EP. Then a scenario study was carried out by using a thermodynamic model to assess the feasibility of recovering Na₂SO₄ from the brine produced by a DWP plant.

1.2 Knowledge gaps and research objectives

1.2.1 Effect of NaCl on the recovery of Na₂SO₄

In an effective crystallization process, with a pure salt solution system, the recovery of aim salt can reach 100%. When reaching the EP, ice and salt are separated in a fixed ratio at the constant temperature, corresponding to the composition at EP. However, the presence of impurities reduces the recovery of salt by directly alter the surface diffusion and incorporation kinetics or indirectly change the solubility. Thus, reduce the purity of the ice product, brings difficulties for the separating work.

Studies about the effect of inorganic impurities on using EFC to recover Na₂SO₄ have been conducted widely. Reddy et al. (2011) recovered Na₂SO₄ (4%) from a reverse osmosis retentate with some impurities (F, Cl, K, Li, Mg, Ca, NO₃ and NH₄) found that concentrated NaCl (20 wt.%) inhibit ice crystallization ⁷. Edward et al. (2016) observed the effect of phosphonate antiscalant (K⁺, Na⁺, P³⁻) during the EFC of Na₂SO₄ ⁸. According to the results from Reddy et al. (2011), the presence of NaCl (20 wt.%) lows the EP of Na₂SO₄.

Though Reddy et al. (2011) had proved that the presence of NaCl depressed the EP of Na₂SO₄-H₂O system ⁷, to what extent this decrease would be, and how the nucleation temperature of ice and Na₂SO₄ are altered are still unknown. Besides, even though Reddy et al. (2010) showed that the crystalline composition was also affected by Na₂SO₄ concentration and NaCl concentration in the solution in a modelling study, no previous study provided quantitative information to what extent this effect would be ⁹. Moreover, the recovery and purity of ice and Na₂SO₄ are influenced by the different pre-treatment process of EFC. To achieve the sequential separation of salts, a proper treatment process needs to be explored.

According to the stated knowledge gaps, the research objectives are:

Investigate the effect of high concentration of NaCl on EFC of Na₂SO₄ from the aspects of temperature and product composition.

Using the thermodynamic model to assess the feasibility of applying EFC to recover Na₂SO₄ from the brine produced by DWP plant with the different pre-treatment process.

1.2.2 Research questions and approaches

Based on state of the art mentioned in Chapter 1.1 Research background, the following four research questions are formulated to meet the research objective stated in Chapter 1.2.1.

- (1) Does the solubility and eutectic concentration of Na_2SO_4 increase or decrease with increasing NaCl concentrations?
- (2) Does the eutectic point of $\text{Na}_2\text{SO}_4\text{-H}_2\text{O}$ system decrease with increasing NaCl concentration?
- (3) How much the ice and Na_2SO_4 recovery in EFC would be with the different pre-treatment process?

1.3 Thesis structure

To answer the above research questions, two research approaches were applied in this study: literature review and laboratory research. According to two research approaches, the thesis was divided into eight chapters.

Chapter 1: Introduction

Chapter 1 gives the general background information of this study and provides the relevant research questions.

Chapter 2: Literature review and theory

The literature presented in Chapter 2 is firstly carried out to understand the underlying mechanisms of EFC technology, and then identifies the gap in the literature that this study intends to fill. As the research continued, the collected experimental data were analyzed and explained based on the literature to ensure the theoretical stringency of the results.

Chapter 3 & 4: Laboratory research and modelling work

To effectively accomplish the research objectives, a series of laboratory work was conducted to collect the solubility data of sodium sulfate. The detailed procedures are presented in Chapter 3. Chapter 4 describes the scenario study process in detail. A thermodynamic model was built up to simulate the continuous mode of EFC process and therefore to investigate the relation of solution concentration and product yields.

Chapter 5: Result and discussions

Chapter 5 describes and explains the study finding of experimental result and simulation result.

Chapter 6: Conclusion

This chapter answers the research questions and lists out the important realizations in the study.

Chapter 7: Research limitations and recommendations

This chapter lists out the limitations of the experiment set-up and the design of the study. Besides, this chapter provides suggestions for future study and application.

Chapter 2 Theory and Literature Review

Relevant background information about EFC technology and impurities studies presented in other researchers' studies that are related to this research are discussed in this chapter. Chapter 3.1 explains the terminologies and concepts in crystallization technology that will be referred to in the following chapters. The fundamentals of EFC are presented in Chapter 3.2. Then Chapter 3.3 presents two operation modes in EFC. Chapter 3.4 includes the current research progress using EFC to recovery Na_2SO_4 . Next, the impurity study and the ice scaling phenomenon are summarized.

2.1 Mechanisms of crystallization

2.1.1 Phase diagram

Phase diagram graphically presents the equilibria between various phases under different temperatures, pressures, and composition. It identifies the equilibrium condition and the presenting phases (solid, liquid and gas) at a certain composition corresponding to a certain temperature ¹¹. In this study, the discussion is within the temperature and composition of solid-liquid equilibria in the binary or tertiary system, the change in pressure is neglectable.

Typical binary temperature-composition phase diagram is shown in Figure 2.1. The graph shows a mixture of A and B, temperature (T), the mole fraction of B (x_B), the number of phases co-exist in equilibria. According to the temperature and concentration of the solution, whether the solution is saturated or diluted can be estimated. The maximum phases the system reaches are three, which is at the EP. Below the solidus line, solid phases are present at all compositions in equilibrium; above the liquidus line, the system is in liquid. More often, the liquidus line is called solubility line ¹¹. In EFC, left part of liquidus line is ice line while the right part is the salt line.

The theoretical yields of each compound can be calculated using the phase diagram. The relative ratios obey the ruler rule:

$$\frac{\text{Weight of salt}}{\text{Weight of complete system}} = \frac{CD}{CF}$$

Equation 1

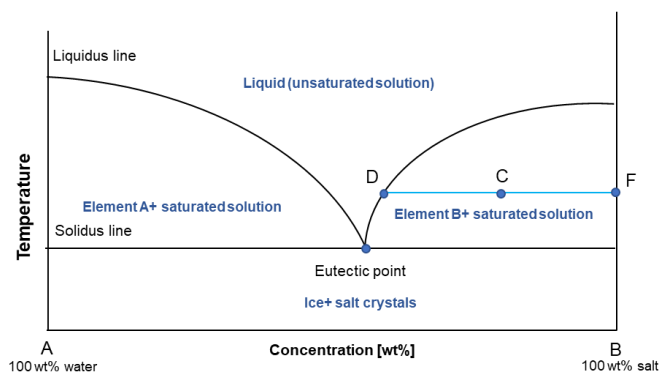


Figure 2.1 Binary phase diagram of element A and B. A mixture of A and B

The concentration of B changes with temperature. Solution composition at A:100 wt% H₂O, B:100 wt% salt.

The phase equilibria in the ternary system is complex. The composition of the system can be plotted in a triangular graph, which is shown in Figure 2.2. The three corners of this triangle represent pure component. The two-phase region is below the arch while across the arch where is the single-phase region.

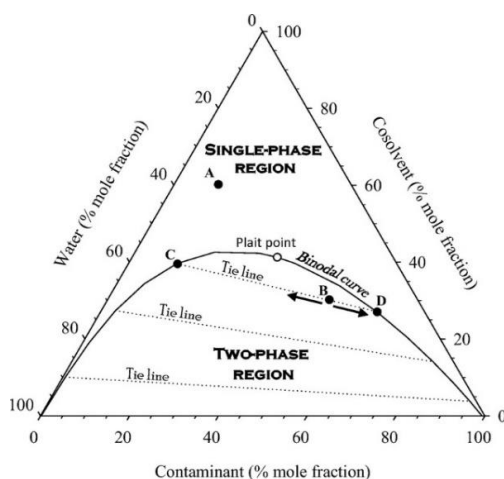


Figure 2.2 phase equilibria in the ternary system ¹⁷

2.1.2 Supersaturation

Supersaturation refers to a condition that solution contains a more dissolved substance in a solvent than it could be under normal circumstance. It is a prerequisite before a solid phase appears in a saturated solution ¹⁰.

2.1.3 Crystallization

Crystals are molecules or atoms bound with highly ordered structure and have a reproducible appearance. Crystallization is regarded as one of the oldest separation and purification technology of human. By screen out the desired product from the mother liquor using this thermodynamically based technology, the applications of crystallization vary from normal life to industries ¹¹.

Supersaturation is the fundamental driving force of crystallization. It is referred to as a solution in which the solute concentration exceeds the equilibrium solution concentration at the given temperature. The dimensionless form of supersaturation is shown in Equation 1.

$$\frac{\mu - \mu^*}{RT} = \ln \frac{a}{a^*} = \ln \frac{\gamma c}{\gamma c^*} \quad \text{Equation 2}$$

Chemical potential (μ), temperature (T), activity (a), activity coefficient (γ) concentration (c). * represents the property at saturation.

2.1.4 Crystal lattice

A crystal lattice is the arrangement of the atoms or molecules that form crystals. As shown in Figure 2.3, the lattice is made up of repeating units ¹².

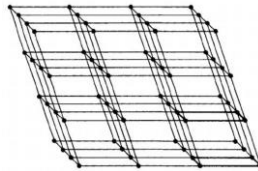


Figure 2.3 A point lattice ¹²

The repeating unit call point lattice, which is used to describe the highly ordered structure of crystals. It can be constructed having unit cells in the regular shape such as square and rectangle, etc. Every point represents a position of an ion.

2.1.5 Nucleation of crystals

A two-steps process is necessary to cultivate crystals. The first is the birth of new crystals from supersaturated solution, known as nucleation. The second is growing the crystals into larger size ¹².

Nucleation is the initial formation of the solids that have characteristics of crystalline. It occurs in solution, vapour, liquid, in which a small number of ions, atoms, or molecules from a site that allows additional particles deposits. Nucleation temperature refers to the temperature when nucleation happens.

Primary nucleation refers to the formation of the first nucleus without introducing crystals ¹³. It is subdivided into heterogeneous or homogeneous nucleation regard on whether the nucleation occurs on the foreign surfaces or not ^{11,12}. Heterogeneous nucleation happens when foreign particles appear in the solution. They orient the formation of the crystal. The surface of a different substance, such as: dust particle and the wall of the reactor, always acts as the centre of a crystal. Homogeneous nucleation is a spontaneous behaviour of a pure and supersaturated solution. Secondary nucleation refers to the crystal nuclei produced from a pre-existing crystal ¹¹⁻¹³. Seeding is the best method to induce crystallization and to prevent excessive nucleation.

2.1.6 Crystal growth

The growth process enlarges the existing nuclei. It is always described as changes in some dimension with respect to time ¹². Usually, there are three ways to express the crystal growth rate: face growth rate, overall mass growth rate, overall linear growth rate.

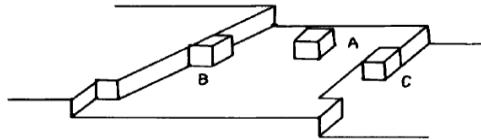


Figure 2.4 A, B, C, three sites molecules can incorporate into the crystal surface

As shown in Figure 2.4, A, B (step) and C (kink) are three possible sites for molecules to incorporate into the crystal surface. Position C is more likely to grow than other positions from the thermodynamic aspect of view because it is bound by three nearest neighbours and has a great chance to become the centre of a crystal.

The driving force of crystallization refers to the supersaturation that makes growth happen ¹⁴. The decrease of free energy in the system related to crystallization promotes the growth of crystals. In the supersaturated solution system, the difference between the chemical potential of the solution phase (μ_c) and the chemical potential of the crystalline phase (μ_m) is the driving force ($\Delta\mu = \mu_m - \mu_c$). This driving force is associated with temperature. When the state is stable, the level of supercooling ($\Delta T = T_m - T$) is the most straightforward and measurable index represents the driving force of crystallization. T , T_m : the temperature at the melting point ¹⁵.

2.1.7 Product characteristics

Crystal structure: Crystal structure describes the ordered arrangement of crystals. Each crystal unit cell has a three-dimensional repeating pattern of its structure ¹⁶.

Morphology: Crystal morphology is termed as shape or habit of crystals. It is an essential factor that determines product quality. Different shape of products has a different dissolution rate.

Crystal size distribution (CSD): Two types of crystal size distribution are density distribution and cumulative distribution ¹². The size and size distribution of the crystalline product partly determine the separation efficiency of the crystallization technology.

Yield: the mass of the salt product or ice product, usually in g/L of feed.

2.2 Fundamentals of EFC technology

EFC is a promising desalination technology. It is established based on the theory that each salt solution has its EP. The EP is a representative equilibrium point in phase diagram where the salt, ice and solution co-exist ¹⁸. With more than twenty-year development, EFC has

shown its potential in RO retentate treatment and salt recovery. It also has been proved to be more energy-friendly than conventional evaporative crystallization ⁶.

EFC borrows the concept that crystals can precipitate from a solution due to the extraction of heat ⁵. In the cooling process, when the solution system reaches its EP, the ice floats on the surface while the salt settles down due to density difference so that they can easily be separated.

This process is presented in Figure 2.5. It is a binary phase diagram for the inorganic compound in a common situation. Phase diagram builds up the foundation of EFC technology. By analysing the solution concentration and temperature in the phase diagram can help to have a better understanding of solubility and prediction of crystalline product composition.

The diagram plots temperature against salt concentration. The left vertical represents 100% ice, whereas the right one is 100% salt. There are four different phases shown in the graph: liquid, ice + saturated solution, salt + saturated solution, ice + salt. When a feed stream with a concentration corresponding to point A enters the crystallizer, at first it is in liquid, and the salt concentration lower than the eutectic concentration. By decreasing the temperature of this mixture, point A will vertically reach point B. Before it reaches point B, the composition of the solution is fixed. When the point touches point B, there will be a small portion of ice in the reactor. After that, the ice keeps freezing, the salt mass is going up along the ice line with decreasing temperature and eventually get to point E, which is at the eutectic temperature and also the critical point of the four phases ^{5,19}. At this time, the system of ice, salt and solution reaches equilibrium. Ice and salt then crystallize simultaneously at supersaturated conditions in the area below point E.

In another situation, when the solution concentration is higher than the eutectic concentration, the cooling process follows the path from C to D and reaches E eventually. Instead of ice, the salt crystal precipitates first. The rest of crystallization behaviour is the same as process A to E.

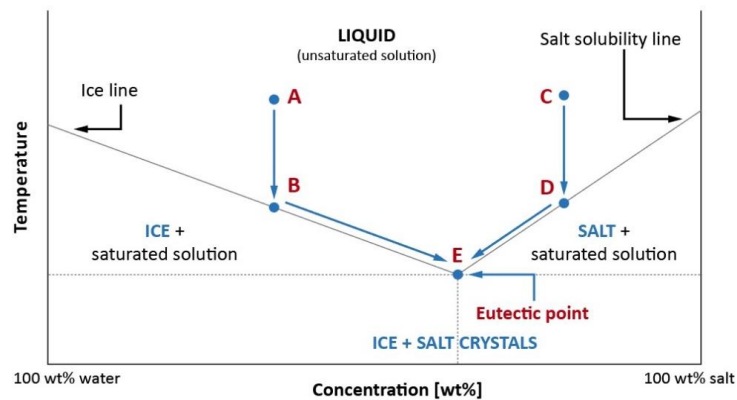


Figure 2.5 A simplest water–salt phase diagram at constant pressure ²⁰.

2.3 Processing modes of EFC

There are two crystallization modes, batch and continuous mode. The selection of mode highly depends on the configuration of equipment and the requirement for the crystalline product ¹².

The traditional batch crystallization process has been adopted widely in chemical, pharmaceutical, photographic and other industries. During the process, the supersaturation of the mother liquor is changed throughout time. The discharge of the product is made only once at the end of the run. Batch cooling crystallization is the most frequent method if the solute solubility changes rapidly with temperature. It has been used widely in the laboratory to examine a large number of operational variables the characteristics in a short time. Though the batch mode has been extensively studied, there still exist some problems. The heat and mass transfer cause severe ice scaling, the complicated operation constraints the consistent ice and crystalline product ¹².

Recently, continuous crystallization has harvested interests from both industry and academia. Compare with the batch crystallization process, one of the most apparent advantages that continuous mode has is that it produces a consistent product specification. The shape and size of the products are even ²¹. The general flow diagram of continuous EFC process is shown in Figure 2.2. In a continuous EFC process, the feed stream is pre-cooled close to the saturation point before flowing into the crystallizer. The temperature in the crystallizer remains constant at sub-eutectic temperature, where the precipitation and growth of ice and salt proceed. The salt crystals and ice are simultaneously separated due to the density difference. Ice floats on the top of crystallizer flow to the ice settling tank then are filtrated and separated with the residual mother liquor. The mother liquor is then recycled back to the crystallizer. Salt crystals, which is obtained at the bottom of the crystallizer, is treated almost the same as ice. After filtration and washing, part of the residual mother liquor is returned to the crystallizer for further crystallization ^{5,22}.

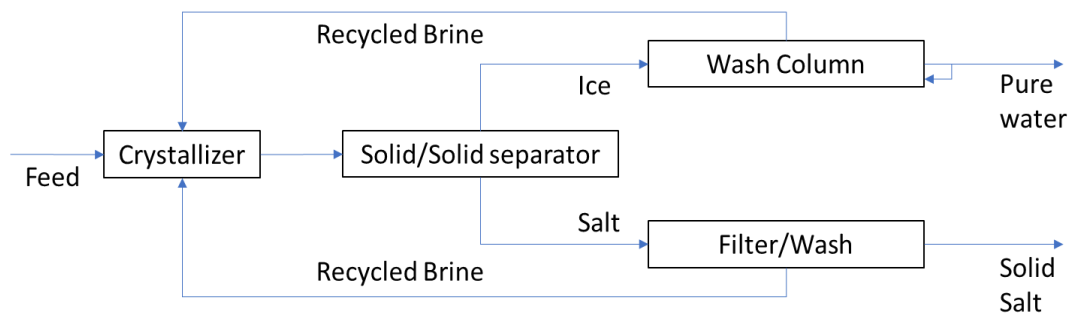


Figure 2.6 Schematic representation of continuous EFC process for the production of pure water and salt ⁴

2.4 Heat transfer in EFC

The heat transfer in a crystalline reactor comprises the heat absorption of coolant, the heat release from the formation of crystals and heat dissipation of scraper and reactor wall, etc. As mentioned in Chapter 2.1.1

The driving force is expressed in term of temperature difference. The heat absorption of coolant is given by Equation 3 and Equation 4. Where c_p is specific heat capacity, ΔT is the temperature change of cooling medium, m is the solution mass flow rate.

$$Q = -Q_{coolant} + Q_{crystallization} + Q_{dissipation} \quad \text{Equation 3}$$

$$Q_{coolant} = mc_p\Delta T \quad \text{Equation 4}$$

2.5 Recover Na_2SO_4 by EFC

Many industrial waste effluents are rich in Na_2SO_4 . For example, the waste streams from textile, glass, mining and kraft pulping industries ²³. There have been several studies focusing on the EFC precipitation of Na_2SO_4 .

Some of the studies focus on the recovery and purity of ice and mirabilite products. Reddy et al. (2011) used batch EFC to treat RO rejection from mining wastewater. It was evaluated that the recovery of water was more than 99%. It also achieved a high purity of Na_2SO_4 (96.4% purity with no washing) ⁶. Then they used cascading EFC to treat textile wastewater and investigated the product yield. It was found that the treatment of EFC brought 95% conversion of the waste stream to ice and $\text{Na}_2\text{SO}_4 \cdot 10\text{H}_2\text{O}$. The relative purity of ice after washing reached 98%, the yield of Na_2SO_4 was 30%, but it could be approved if the feed stream was more concentrated.²⁴.

Some of the studies focus on the exploration of crystallization kinetics. Edward et al. (2016) explored the effect of a phosphonate-based antiscalant on the crystallization kinetics of ice

and mirabilite in a continuous EFC process. It was concluded that the presence of antiscalant decreased the ice nucleation rate, but there was no effect on mirabilite morphology⁸. Emily et al. (2017) evaluated the influence of phenol on the crystallization kinetics of ice and mirabilite during batch EFC process²⁵.

There are some other studies centralized on the improvement of technique. Hasan et al. (2017) recovered Na₂SO₄ with air-cooled (non-stirred) batch EFC and analyzed the influence of different factors and operating conditions²⁶. It was investigated that the recovery of Na₂SO₄ was 11.8 wt%. Jooste (2016) searched for the operating factors that affected the ice scaling in continuous EFC of Na₂SO₄²⁷.

2.6 Impurity Studies in EFC

The previous studies about EFC concentrated more on process parameters, design work and crystal size while the systematic study about the intervenes of impurities is relatively lacking²⁸.

Raymond et al. (2003) performed EFC on an industrial KNO₃-HNO₃-H₂O system with a slight amount of impurities (Ca²⁺, Mg²⁺, Na⁺, NH₄⁺). It was found the main impurities stuck on ice surface was K⁺ and could be washed off²⁹. Lewis et al. (2010) and Reddy et al. (2010) found that the existence of multi-ions (F, Cl, K, Li Mg Ca NO₃) depressed the EP of Na₂SO₄-H₂O system. With the presence of a high concentration of NaCl (20 wt%), the recovery of mirabilite reached 90% at a temperature of -15°C. This result implied a sequential removal of salts from brine^{7,30}. Besides, Edward et al. (2016) investigated the effect of phosphonate antiscalant on the EFC Na₂SO₄-H₂O. Both ice and salt showed an increasing trend in terms of growth rate with a higher concentration of antiscalant. The nucleation rate of ice decreased, but the nucleation rate of mirabilite did not show noticeable change⁸. Debbie et al. (2019) studied the effect of impurities (Ca²⁺, Mg²⁺ and Cl⁻) on ice scaling in batch EFC of Na₂SO₄-H₂O system. It was found that the ice scaling tendency was reduced due to the electrostatic interaction between the solute ions and the electropositive ice surface³¹. Besides, Chen et al. (2019) recovered Na₂SO₄·10H₂O and NaE (Sodium erythorbate) sequentially from pharmaceutical wastewater through EFC. This research is one of the few studies reporting on organic salt recovery with EFC. The results showed that negligible amounts of impurities (Al, Si, S, Cl) adhered on the Na₂SO₄·10H₂O surface, but incorporated into NaE³².

In terms of the effect of organic impurity on EFC process, limited research has been done³². Only Becheleni et al. (2017) worked on the application of EFC to recover Na₂SO₄ from synthetic petrochemical saline solution with the presence of phenol. It was found that phenol improved salt growth rate and reduced nucleation rate²⁵.

2.7 The mechanism of impurities incorporated into crystallization

There are two general mechanisms that impurities incorporated into the crystals during the crystallization process: (1) the adsorption of impurities into the crystal lattice or onto the crystal surface (2) solvent inclusion in the crystals.

1. Adsorption of impurity onto the crystal:

(1) Thermodynamic adsorption of impurity

The formation of intermolecular bonding drives this thermodynamic adsorption. The bonding causes a release of the least free enthalpy energy corresponding to the equilibrium condition between the mother liquid and impurity.

(2) Kinetic adsorption of impurity onto the crystal

The kinetically driven impurity adsorption is another kind of adsorption that results in the impurities adhere to the crystals. This kind of adsorption affects the total thermodynamic adsorption rate of impurity at each point in the crystallization. It was found that the growth rate is decreasing with a rising impurity concentration. If the crystals grow slowly, there would be a different amount of impurities in the crystals. The effect of impurity concentration on the adsorption is summarized as below:

Low concentration: at low impurity concentration, the kinetic-driven adsorption is in predominant. The thermodynamic-driven adsorption is negligible.

High concentration: at the high impurity concentration, the crystal surface is a desirable site for the impurity to adhere on. This adsorption is a thermodynamic-driven process. The formation of the adsorption layer is preferable when large-sized impurities present in the system. Because the interaction between the large inhibiting species and an adsorption site is weak, another issue caused by the high concentration of impurity could be the nonuniform adsorption of impurities, it leads to irregular growth. Part of the crystals follow the growth mechanism and have adsorption, while the rest are entirely blocked by impurities. In general, the thermodynamically driven impurity adsorption induces the incorporation of an impurity into the target crystal lattice ³³.

2. Solvent Inclusion of Impurity into the Crystal

The solvent can be incorporated as an impurity via three mechanisms: (1) thermodynamic and kinetic adsorption on either crystal lattice or surface, (2) liquid inclusion into the growing crystal in three-dimensional defects, and (3) solvent entrapment in between crystals.

Overall, the effect of impurities on crystal growth is hard to predict. The operating condition, the solution composition and other factors affect this process.

2.8 Ice scaling in scraped wall crystallizer

Ice scaling formation in EFC is a complex process. There exists an adhesive force between ice crystals and cold heat exchanger surface. If ice scaling is not prevented, a scaling layer will form on the heat exchanging walls resulting in a substantial decrease of heat transfer rates ³⁴.

Chapter 3 Experimental study on the effect of NaCl concentrations

3.1 Materials

The Na_2SO_4 (sodium sulfate) powder used in this study was purchased from Merck KGaA, Germany. The NaCl (sodium chloride) was purchased from Avantor Performance Materials B.V., the Netherlands.

As shown in, a 5 L scraped cooled wall crystallizer (SCWC) with triple-layered glass filled with liquid coolant and monitoring device will be used for solubility experiments. The inner wall of the SCWC was scraped using a scraper made of high-density polyethylene. During the experiment, the rotate speed of the scraper was set at a fixed 90 rpm. The solution temperature was controlled and monitored by the thermostatic unit LAUDA RP4080 CW. The solution conductivity was measured continuously by Consort C3010 multi-parameter analyzer for every 5 seconds. The data of stirrer refrigerated, water bath circular and conductivity meter were delivered to a computer in line. For a more detailed explanation of the equipment, refer to Appendix A.

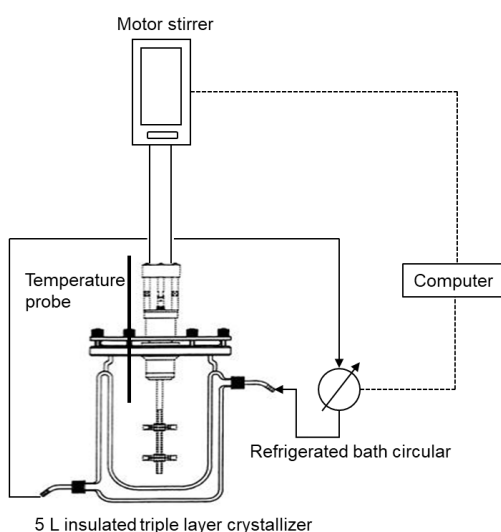


Figure 3.1 Experimental set-up for solubility experiments

A 5 L triple-layer jacketed crystallizer was connected with a motor stirrer, temperature probe and refrigerated bath for the cooling process. All of these pieces of equipment can be controlled by the computer.

3.2 Experimental design and reagents

To determine the salt line, seven batch experiments were carried out. Each time, the same 5 L of aqueous Na_2SO_4 solution with the composition of 175 g/L was prepared, but a different amount of NaCl in terms of 0, 25, 50, 75, 100, 150, 200 g/L was added respectively.

To determine the ice line, 5 L of aqueous Na_2SO_4 solutions with concentrations of 0.0025, 0.005, 0.01, 0.015, 0.02, and 0.025 g/L were prepared respectively. Different amount of NaCl with respect of 0, 25, 50, 75, 100, 150, 200 g/L was added into the prepared Na_2SO_4 solution accordingly. The experiment procedures are described in detail in Chapter 4.3.

3.3 Experimental procedure

The experimental procedure for investigating the effect of NaCl on phase equilibria of $\text{Na}_2\text{SO}_4\text{-H}_2\text{O}$ system is summarized in Figure 3.2 and Figure 3.3. The first half part of the solubility experiment was conducted using a 2 L SCWC, and the later part was conducted in a 5 L SCWC. Except that, all the experimental conditions were the same. The concentration of both Na_2SO_4 and NaCl in these two reactors were not affected. The agitation speed was set to 80 rpm for mixing well. The binary phase diagram of $\text{Na}_2\text{SO}_4 - \text{H}_2\text{O}$ was determined as follows:

Salt line: The batch experiment was carried out to determine the Na_2SO_4 solubility line with the presence of NaCl. The 5 L SCWC was filled with 5 L aqueous solution contained 0.175 g/mL Na_2SO_4 . Each time, different concentrations of NaCl (0, 25, 50, 75, 100, 150, 200 g/L) were added to the Na_2SO_4 solution respectively. The temperature of cooling liquid was adjusted to keep the starting temperature inside the crystallizer at 18°C. The solution was saturated at this temperature according to the literature. Then the cooling process started, Na_2SO_4 began to precipitate during this period. About 30 mL of solution samples were taken by a 10 mL syringe for every ten minutes until the solution reaches the EP of $\text{Na}_2\text{SO}_4 - \text{H}_2\text{O}$. The sampling temperature was recorded by a temperature probe. All the samples were filled by a 0.2 μm filter. This experimental process is summarized in Figure 3.2.

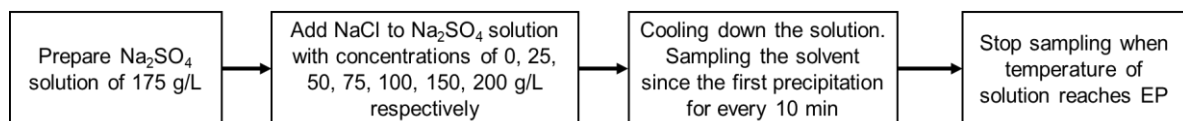


Figure 3.2 Experimental procedures to determine the salt line

Ice line: The batch experiment was conducted to determine the saturation point of the ice line in the phase diagram at the same concentration of Na_2SO_4 with the presence of different concentrations of NaCl. Each time, the 5 L SCWC was filled with 5 L aqueous solution contained a particular concentration of Na_2SO_4 (0.0025, 0.005, 0.01, 0.015, 0.02, and 0.025 g/L respectively). At first, no NaCl was added, the solution was cooled down till almost reached 0 °C. Then about 5 g ice seed was added. A 30 mL of solution sample was taken when the first ice crystal was observed. All the samples were filtrated by a 0.2 μm filter. The temperature at

this point was recorded. Later on, 125 g NaCl was added. This extra adding made the concentration of NaCl in compliance with 25, 50, 75, 100, 150, 200 g/L for each time accordingly. The temperature in the crystallizer was increased to speed up the dissolution and then decreased again. The above steps were repeated until the first crystal turned to be salt. This experimental process is summarized in Figure 3.3.

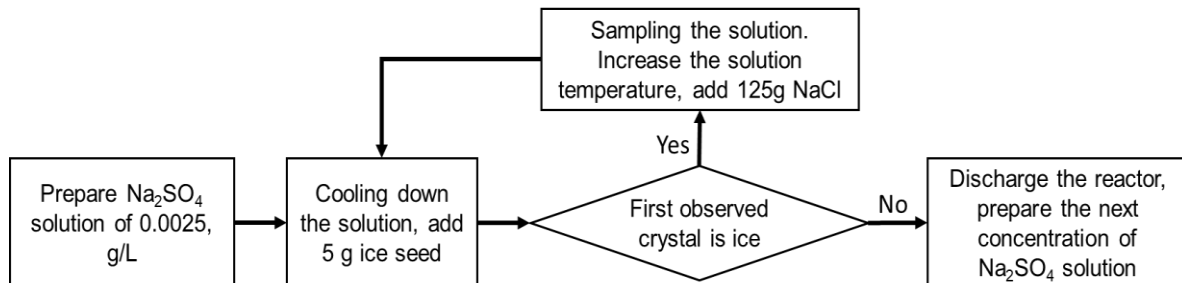


Figure 3.3 Experimental procedures to determine the ice line

3.4 Measurements

3.4.1 Temperature

The temperature of the feed solution (T_1), bulk liquid (T_2), coolant inlet (T_3) and coolant outlet (T_4) were measured with platinum resistance thermometers (Pt100), with an accuracy of ± 0.01 °C. The flow rate of the cooling liquid was kept constant at 1500 kg/h. The thermometers were connected to online data recording software.

3.4.2 Concentration

According to the results from the pre-experiment, the whole cooling process (from the first appearance of crystal till equilibrium) took about 90 minutes. Residual mother liquor samples were taken by a 30 mL syringe fitted with a 0.2 μm filter. The ion elemental analysis of Na^+ , SO_4^{2-} and Cl^- for liquid phases was performed on Ion Chromatography (IC).

3.4.3 Stirring torque

The stirring force required to rotate the scrapers was measured as torque by a sensor. Stirring torque is a parameter that associate with ice scaling.

Chapter 4 Modelling study about continuous EFC of Na₂SO₄

The phase equilibria is the foundation of EFC process. The solubility data of a multi-component brine at the low-temperature range is in limited availability. The phase diagram comprises more than four components is impractical. Therefore, a thermodynamic modelling tool was used to accurately predict phase equilibria and kinetic change in electrolyte solution over a broader range of temperature.

OLI Stream Analyser is such a modelling tool that investigates EFC-related equilibria. OLI adapts framework of Bromley – Meissner, Pitzer, Helgeson for those excess terms. Particularly, with a given amount of solvent and solute, the composition of the solution and the precipitated phase and under a certain temperature can be predicted. The recoveries and the yields of each compound can also be known. From the aspect of accuracy, D.Randall (2011) compared OLI with the extending UNIQUAC model. Results showed that OLI had higher coincidence with experimental data ⁹.

In this chapter, the solubility curves of Na₂SO₄ – H₂O system with different addition of NaCl were determined based on the simulation results from OLI Stream Analyser. These results were compared with the experimental data. Then the scenario study was carried out to investigate the influence of pre-treatment on continuous EFC of Na₂SO₄.

4.1 OLI Stream Analyser modelling procedure

Figure 4.1 shows the thermodynamic modelling procedure of OLI Stream Analyser. The blocks give the steps during the simulation. The simulation was achieved by inputting corresponding data in either of the first three blocks. If only have ion data, to get the simulation results needs to go through all of three kinds of analysis. Ion data was input at 'Brine Analysis', the output of which gave conditions of pH, alkalinity, density, etc. Also, at this step, the input ion data would be reconciled. Those outputs could be the input data of 'Water Analysis', and the production of "Water Analysis" could be the input data of "Stream Analysis".

In the interpretation and modification step, there were three models helping for the optimal calculation, which are shown in Table 4.1. In this study, the MSE model was chosen. It is

capable of a complex system containing electrolytes and non-electrolytes over a broad concentration range and at a variety of temperatures. Furthermore, it is especially good at calculating salt solubility that reaches the fused salts limit or at a critical temperature.

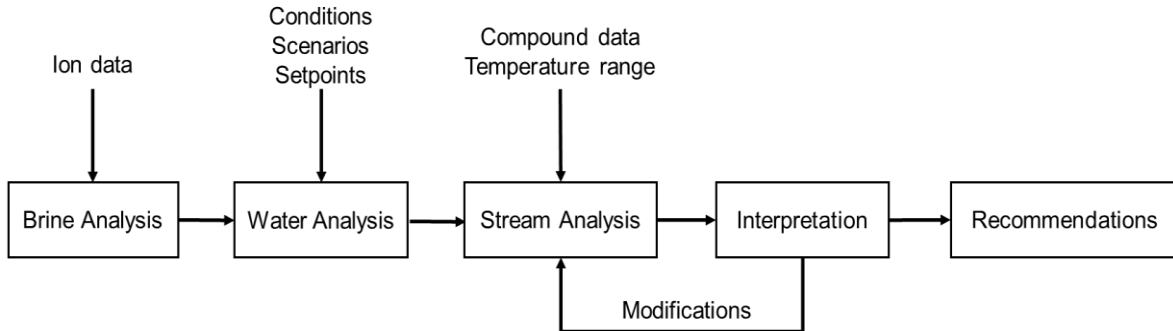


Figure 4.1 Thermodynamic modelling procedure in OLI Stream Analyser

Table 4.1 Three models provided in OLI Stream Analyser

Model Name	Aqueous (AQ)	Mixed Solvent Electrolyte (MSE)	MSE-SRK
Scope of Application	<p>Corrosion rate calculations</p> <p>Mineral scaling during oil and gas production</p> <p>Flue gas scrubbing using lime, caustic, or limestone</p>	<p>Salt solubility that reaches the fused salts limit</p> <p>Conditions approaching critical temperature</p> <p>Electrolytes dissolved in non-aqueous solvents</p>	<p>High-pressure upstream oil and gas production environments</p> <p>Predicting the effects of salts on the solubility of acid gases in aqueous solutions</p>

MSE model evaluates the excess Gibbs energy. This is a function of three energy terms: (1) long-range electrostatic interactions. (2) specific ion-ion and ion-molecule interactions. (3) short-range interactions³⁵.

$$\frac{G^{ex}}{RT} = \frac{G^{ex}_{LR}}{RT} + \frac{G^{ex}_{II}}{RT} + \frac{G^{ex}_{SR}}{RT} \quad \text{Equation 5}$$

Similarly, the activity coefficient is given by:

$$\ln v_i = \ln v_i^{LR} + \ln v_i^{MR} + \ln v_i^{SR} \quad \text{Equation 6}$$

(1) The long-term interactions are quantified using the Pitzer-Debye-Hückel formula:

$$\frac{G^{ex}_{LR}}{RT} = -\left(\sum_i n_i\right) \frac{4A_x I_x}{\rho} \ln \left(\frac{1 + \rho I_x^{1/2}}{\sum_i x_i \left[1 + \rho(I_{x,i}^0)^{1/2}\right]} \right) \quad \text{Equation 7}$$

(2) The medium-range interactions are calculated from an ionic strength-dependent, symmetrical second virial coefficient-type expression; this is key to modelling concentrated electrolytes:

$$\frac{G^{ex}}{RT} = -\left(\sum_i n_i\right) \sum_i \sum_j x_i x_j B_{ij}(I_x)$$

Equation 8

(3) The short-range interaction uses the UNIQUAC model to calculate.

$$\frac{G^{ex}_{SR}}{RT} = \frac{G^{ex}_{UNIQUAC}}{RT} = \frac{G^{ex}_{combinatorial}}{RT} + \frac{G^{ex}_{residual}}{RT}$$

Equation 9

With:

$$\frac{G^{ex}_{combinatorial}}{RT} = -\left(\sum_i n_i\right) \left[\sum_i x_i \ln \frac{\phi}{x_i} + \frac{Z}{2} \sum_i q_i x_i \ln \frac{\theta_i}{x_i} \right]$$

Equation 10

And:

$$\frac{G^{ex}_{residual}}{RT} = -\left(\sum_i n_i\right) \left[\sum_i q_i x_i \ln \left(\sum_j \theta_j \tau_{ij} \right) \right]$$

Equation 11

4.2 Effect of NaCl concentration on the solubility of Na₂SO₄

This study was exploratory and interpretative. The thermodynamic model was used to verify the experimentally determined Na₂SO₄-H₂O phase diagram. Then NaCl was substituted to KCl to further inquire into the interaction between the ions. The model input is shown in Appendix B, Table A1.

4.3 A scenario study: effect of pre-treatment on the product yield and recovery in continuous EFC of Na₂SO₄

In this scenario study, the main issue was to test the influence of various pre-treatment process during the EFC of Na₂SO₄. RO concentrate was from a DWP plant. Figure 4.2 describes the conventional treatment procedures of the brine. The stream was first fed to a TOC removal unit, then passed through NF. The NF concentrate will be fed to an EFC unit wherein the ice and salt would be separated and recovered.

Benchmark experiments at several sampling points were done to collect the stream data. It was concluded that Na₂SO₄ was the most potential salt that can be extracted by EFC. Even with the limited result, a necessary adjustment of the treatment process was foreseen. The concentration of Na⁺ and SO₄²⁻ were various at the influent and effluent of each unit. The presence of other interfering ions such as Cl⁻ and HCO₃⁻ brought more uncertainties in

crystallization. Thus, it still did not decide to extract which stream or a mixed stream as the feed of EFC.

To sum up, it was essential to study the effluent of crystallizer carefully and consider the possible pre-treatment options or making assumptions of the process to test the feasibility of using EFC to recover Na₂SO₄.

The current data included the influent and rejection of NF when TOC unit was open and off. Four scenarios with different routines were put forwarded based on the provided data. The simulations started from 5°C with 0.25°C interval till -25°C by using the ion concentration data as the input in OLI Analyser. Each time, the stream input was with 1kg of solvent, and all the concentration was calculated based on mass. In Chapter 5 Results and discussions, the figures only present the shorter temperature range. Because when the main salt compound of the solution system reaches its EP, without the interference of a high concentration of organic synthesis, the temperature of the solution does not change a lot. A quite low temperature of the solution is theoretically accessible but difficult to achieve in reality. The recovery and yield of ice and mirabilite were calculated based on the input ion information and final simulation output.

4.3.1 Effects of different Na₂SO₄ concentrations in EFC

Before introducing the real brine composition to the model, a simulation with only Na₂SO₄ was first done to investigate how the Na₂SO₄ yield changed with its concentration in a continuous EFC process. This simulation lays the foundation of the following scenario study. In this simulation, the temperature ranged from 0°C to the EP of the Na₂SO₄-H₂O system. The ion information as model input is shown in Appendix B, Table A3.

4.3.2 Effect of NaCl concentrations on the recovery of Na₂SO₄ and ice

Before introducing the real brine composition in the model, a simulation with Na₂SO₄ and NaCl was first done to investigate the effect of NaCl on the ice and Na₂SO₄ yield in a continuous EFC process. The temperature ranged from 0°C to the EP of the Na₂SO₄-H₂O system, which depended on the concentration of NaCl. The ion information as model input is shown in Appendix B, Table A4.

4.3.3 Scenario 1: RO-NF-EFC

This scenario is the main scheme of treatment at present. As shown in Figure 4.2, the RO retentate directly goes to NF, then the concentrate of NF acts as a feed of EFC. The detailed ion data is shown in Appendix B, Table A5.

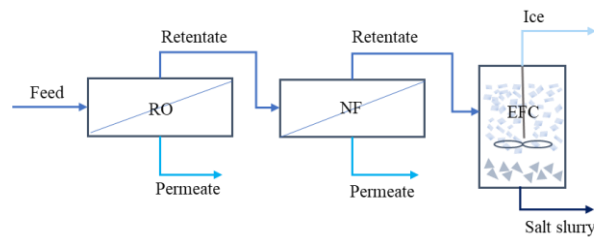


Figure 4.2 Process diagram of scenario 1

4.3.4 Scenario 2: RO-TOC-NF-EFC

In this scenario, the treatment process of brine was different from the brine in scenario 1. The brine will first be fed to TOC removal unit to remove the organics. At the unit, the addition of sulfuric acid introduces a large amount of sulfate. Then the organic-free stream will go to NF unit. Then, NF concentrate is sent to the EFC unit. Figure 4.3 gives the process diagram. Table A6 shows the ion information of NF concentrate after TOC removal unit.

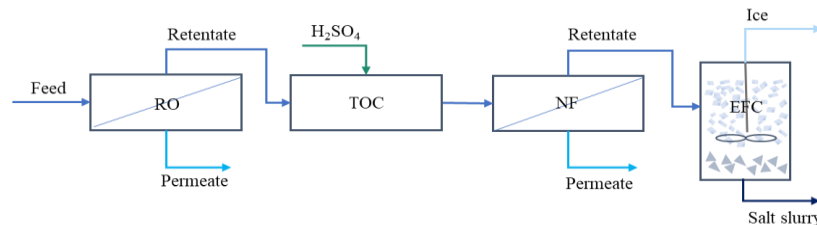


Figure 4.3 Process diagram of scenario 2

4.3.5 Scenario 3: RO-TOC-EFC

In this scenario, the effluent of TOC removal unit was directly linked with EFC. Figure 5.4 and Table 0.11 provide the process and ion information.

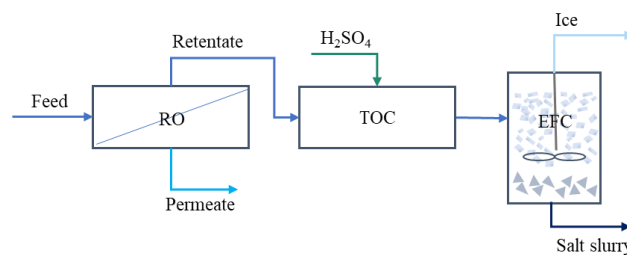


Figure 4.4 Process diagram of scenario 3

4.3.6 Scenario 4: RO-TOC-NF-RO-EFC

Figure 5.6 provides the process information in this scenario. In terms of ion information, the raw data of the EFC feed as RO retentate was unknown. But the NF concentrate was shown in Appendix B, Table 0.7. Thus, software provided by Dupont water solution called WAVE was used for calculating the concentration of RO retentate before EFC by using the NF

concentrate data. The assumption of 70% TOC removal and 70% water recovery was adopted in WAVE when estimating RO retentate concentrations.

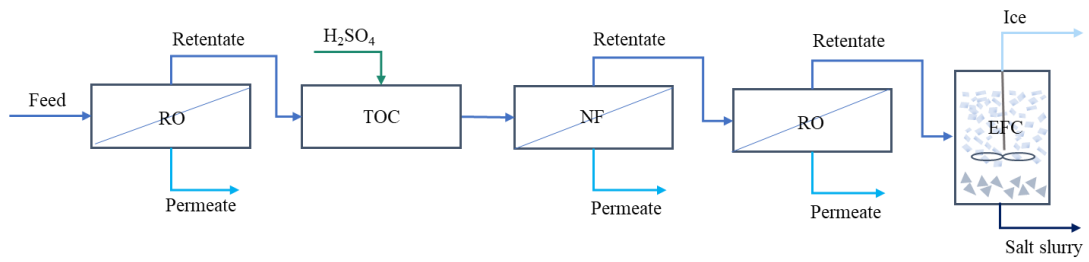


Figure 4.5 Process diagram of scenario 4

Chapter 5 Results and discussions

This chapter presents and discusses the research findings of the research questions stated in Chapter 1 and the consistency to the previous studies catalogued in Chapter 2. The discussion can be divided into two aspects. In Chapter 6.1, the experimental result about the effect of NaCl on the solubility of Na₂SO₄ will be discussed and compared with the OLI modelling predicted result. The error between the experiment and modelling work and the possible reasons that led to the error are summarized. The effect of NaCl on the EP and eutectic concentration of Na₂SO₄-H₂O system was compared with the effect of KCl. In Chapter 6.2, the result of the scenario study is presented. Effects of different pre-treatment processes on the separation of Na₂SO₄ by EFC process were evaluated. The modelling predicted recovery and yield of crystalline product in four scenarios was calculated and compared.

5.1 Effect of high concentration NaCl on EFC of Na₂SO₄ from the aspects of temperature and product composition

5.1.1 Na₂SO₄ - H₂O binary phase diagram

The experimentally determined binary phase diagram of Na₂SO₄-H₂O system with different concentrations of NaCl (0~200 g/L) is shown in Figure 5.1. Each point on this phase diagram represents a saturation point of Na₂SO₄ at a certain temperature.

It can be found that NaCl made the supersaturation of Na₂SO₄ decrease significantly. However, this decreasing trend became less with increasing NaCl. When NaCl concentration reached 150 g/L and 200 g/L, the salts curves were almost superimposed on each other. Except for the pure Na₂SO₄ salt line, the other salt fitting curves conformed to the logarithmic distribution with R² values greater than 0.99. This reflected that the solubility of Na₂SO₄ was more sensitive at the high-temperature range and changed less dramatically at the low-temperature range. The detailed fitting functions and solubility results are shown in Appendix C.

The ice curves (left part of the saturation curve) in Figure 5.1 showed an overall downward tendency and became narrow with increasing concentration of NaCl. At the same concentration of Na₂SO₄, the nucleation temperature of ice became lower with increasing concentration of NaCl. Moreover, the ice line was steadier than the salt line, it reflected that

the solubility change with respect of temperature on the same freezing line was more significant. So, when the solution was quite diluted, the solubility changing with temperature was more sensitive.

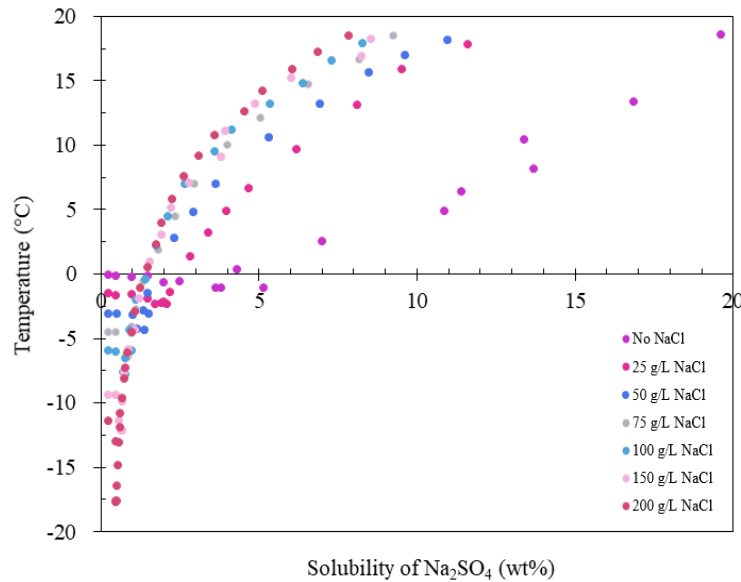


Figure 5.1 Binary phase diagram of Na_2SO_4 - H_2O system changes with NaCl concentrations determined by experiment

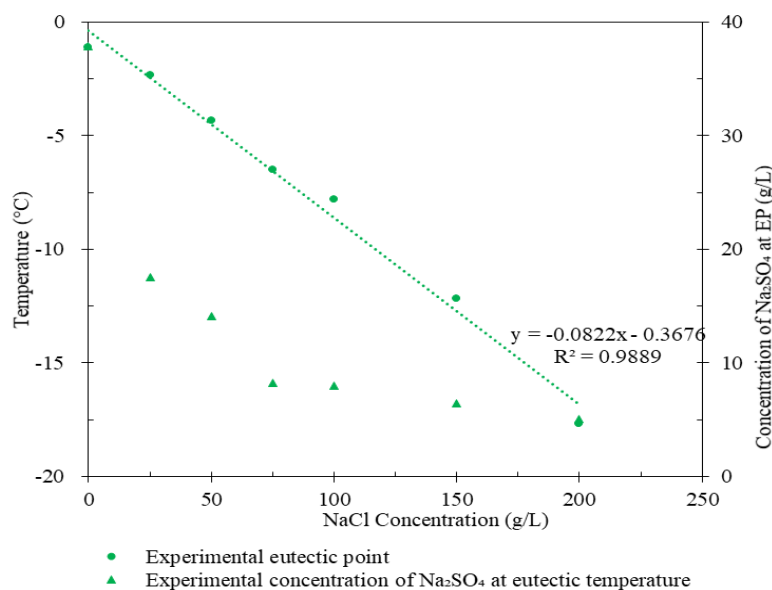


Figure 5.2 EP of Na_2SO_4 - H_2O system and eutectic concentration of Na_2SO_4 with different NaCl concentrations obtained by experiment

Figure 5.2 presents the EP of Na_2SO_4 - H_2O system and the concentration of Na_2SO_4 at EP at different NaCl concentrations. The data was extracted from Figure 5.1. The EP of aqueous Na_2SO_4 solution with no extra addition of NaCl was -1.116°C with a solubility of 4.2 wt%. This result was in a good agreement with the reported values from the literature that EP varied from -1.1 to -1.2°C and solubility of Na_2SO_4 from 3.8 to 4.2 wt% ^{7,8}. With extra NaCl, the EP showed a downward trend, gradually depressed from -2.34°C to -17.67°C . The corresponding

solubility of Na_2SO_4 dropped from 4.2 wt% to 0.5 wt%. The depression of EP with different concentrations of NaCl showed a linear fitting trend with $R^2 = 0.986$. Thus, it was expected that the presence of the NaCl would depress the freezing point of H_2O in hypoeutectic Na_2SO_4 aqueous solutions in proportion to the impurity concentration.

The probable reason resulted in the linear depression of the EP was the common ion effect. Both NaCl and Na_2SO_4 have Na^+ , when two salts containing the same ions dissolve in water, both of their solubility decreases. Besides, with higher salinity, more water molecules act as a hydration shell, and less free water is available as the solvent.

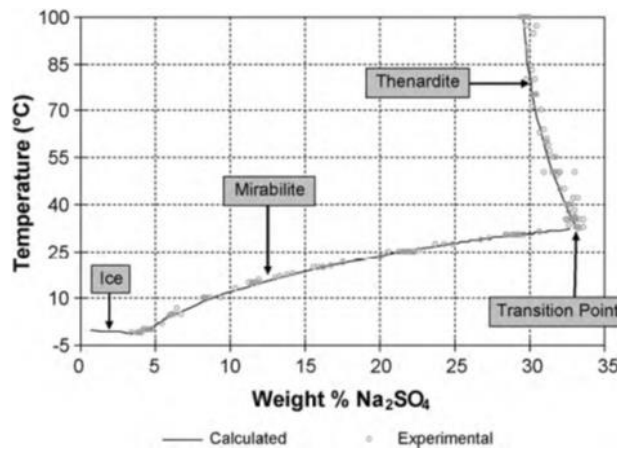


Figure 5.3 Binary phase diagram for $\text{Na}_2\text{SO}_4\text{-H}_2\text{O}$ showing regions of stable phases ³⁰

According to Thomson (presented in Figure 5.3), Na_2SO_4 exists in three forms of the hydrate ³⁰. When the temperature is below 32.27°C , all the $\text{Na}_2\text{SO}_4 \cdot 7\text{H}_2\text{O}$ (Thenardite) transfers to $\text{Na}_2\text{SO}_4 \cdot 10\text{H}_2\text{O}$ (Mirabilite). From one hand, the mirabilite was the dominant crystalline of Na_2SO_4 at low temperature. The formation of mirabilite took water molecule from solution. From another hand, the solubility of NaCl keeps at a relatively stable number before temperature drops to -20°C ³⁶.

To further explore if the common ion effect is the only reason led to the decreasing solubility of Na_2SO_4 , the solubility at of Na_2SO_4 at two temperature points was deduced by using the logarithmic fitting functions in Origin. The ionic concentrations were calculated.

At equilibrium condition under the same temperature, the solubility product equilibrium constant (K_{sp}) is in a fixed value:

$$K_{\text{Na}_2\text{SO}_4} = [\text{SO}_4^{2-}] [\text{Na}_i]^2 \quad \text{Equation 12}$$

After adding NaCl:

$$K_{\text{Na}_2\text{SO}_4} = [\text{SO}_4^{2-}] [\text{Na}_i + \Delta\text{Na}]^2 \quad \text{Equation 13}$$

Where Na_i is the initial concentration of Na^+ .

The calculated value of $K_{\text{Na}_2\text{SO}_4}$, the detailed fitting functions and ion concentration data at 0 °C and 5 °C are presented in Table A9 and Table A10, respectively. It can be observed that the consistency of $K_{\text{Na}_2\text{SO}_4}$ was better when NaCl concentration was larger than 7.5%. When the concentration was below 7.5%, the fitting curve was not as accurate as it of the higher concentration.

5.1.2 Comparison of experimental phase equilibria with modelling results

Figure 5.4 shows theoretical phase diagram of $\text{Na}_2\text{SO}_4\text{-H}_2\text{O}$ system under different NaCl concentrations obtained by using OLI Analyser. Figure 5.5 depicts the trend about how the EP and the eutectic concentration of Na_2SO_4 changed with changing NaCl in the experiment and in the thermodynamic model. The theoretical EP of pure $\text{Na}_2\text{SO}_4\text{-H}_2\text{O}$ system was -1.15 °C, which was almost the same as the experimental value and was comparable to the other EFC modelling study ²⁷. However, after adding NaCl, the theoretical EPs were all higher than the experimental results while the theoretical Na_2SO_4 concentrations at EP become lower than experimental ones. The reason led to the gap might be that the experiment system was unseeded, the nucleation temperature of ice is usually lower.

Error analysis:

The error between the experimental result and the simulation result was calculated and shown in Table A11. It can be observed that at the same temperature, the higher concentration of NaCl resulted in a larger error. At the same concentration of NaCl, the lower temperature resulted in a more significant error. From one aspect, the fitting curve might not fit the experimental data perfectly at the low temperature, so that caused more significant error compared with the high-temperature range. From another aspect, a large amount of mirabilite was precipitated, accumulated and floating in the reactor when the temperature went down, which made the sampling of the solution more difficult to proceed. Although the syringe used for sampling was covered by a filter, it was inevitable that mirabilite and ice crystals were mixed with the solution. Thus, the detected ion concentration of the saturated Na_2SO_4 solution by IC went up, leading to the error. Another reason might be that the experiments were conducted in an unseeded system. The induction time was significantly prolonged compared with the seeded system, and therefore the nucleation temperature was lower.

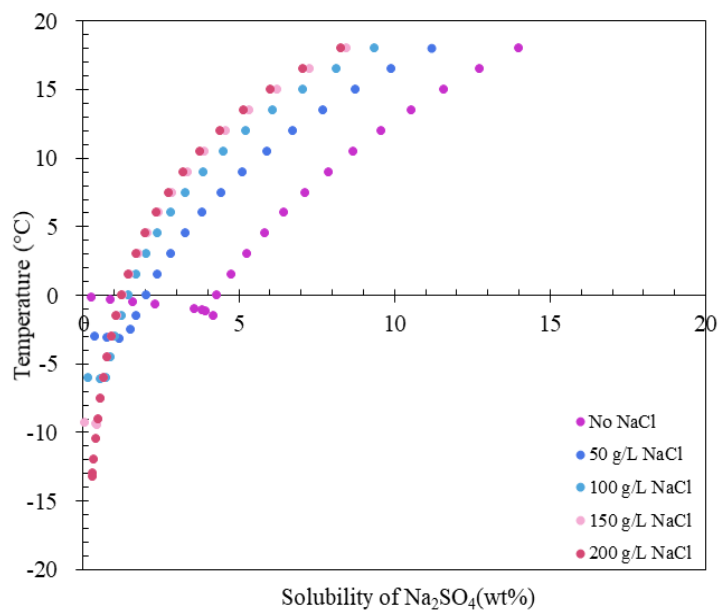


Figure 5.4 Theoretical binary phase diagram of Na₂SO₄- H₂O system changes with NaCl concentrations

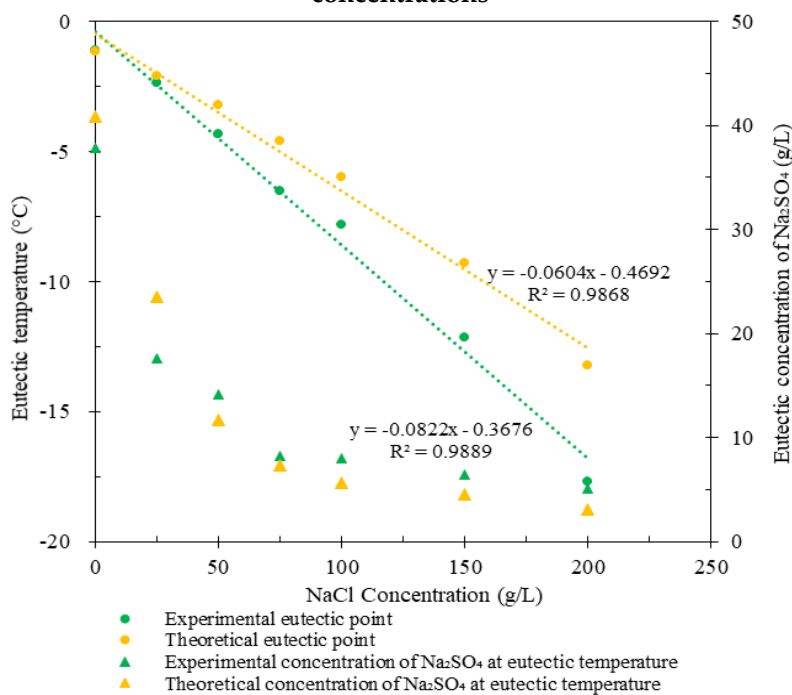


Figure 5.5 The change of the Na₂SO₄- H₂O system EP and eutectic concentration with different addition of NaCl (0-200 g/L)

5.1.3 Comparison of the effect of salt with common ion and uncommon ion on the solubility of Na₂SO₄

In order to further demonstrate the effect caused by salt on the solubility of Na₂SO₄, the same simulation was conducted with the salt that did not contain the common ion with Na₂SO₄. The outcome was compared with the result of NaCl.

The simulation results of adding KCl to the $\text{Na}_2\text{SO}_4\text{-H}_2\text{O}$ system are shown in Figure 5.6 and Figure 5.7. In contrast with the effect of NaCl, the solubility of Na_2SO_4 increased with the additional KCl concentration. The EP of $\text{Na}_2\text{SO}_4\text{-H}_2\text{O}$ system was depressed. When the concentration of NaCl reached 150 g/L, the curve had an inflexion point. It was due to the formation of $\text{KCl}\cdot\text{H}_2\text{O}$ at about 1.5°C . Part of the H_2O was taken from the solution system.

The phenomenon caused by KCl can be explained by salting in effect. When two electrolyte that does not have the same ions, due to the increase in the total concentration of ions in the solution, the interaction between ions is strengthened, which reduces the chance that the anion and cation being dissociated. So the ion concentration increases accordingly, and the degree of dissociation increases. Moreover, NaCl is more covalent than KCl; KCl is more ionic than NaCl. H_2O molecule is a polar solvent. An ionic compound is more soluble in the polar solvent. So KCl is more soluble than NaCl in the water. And thus, strengthen the salting in effect.

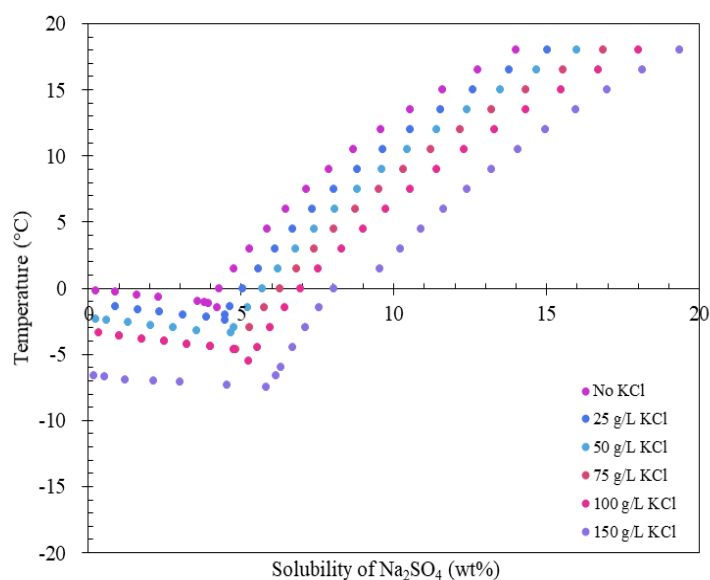


Figure 5.6 Theoretical binary phase diagram of $\text{Na}_2\text{SO}_4\text{-H}_2\text{O}$ changes with KCl concentrations

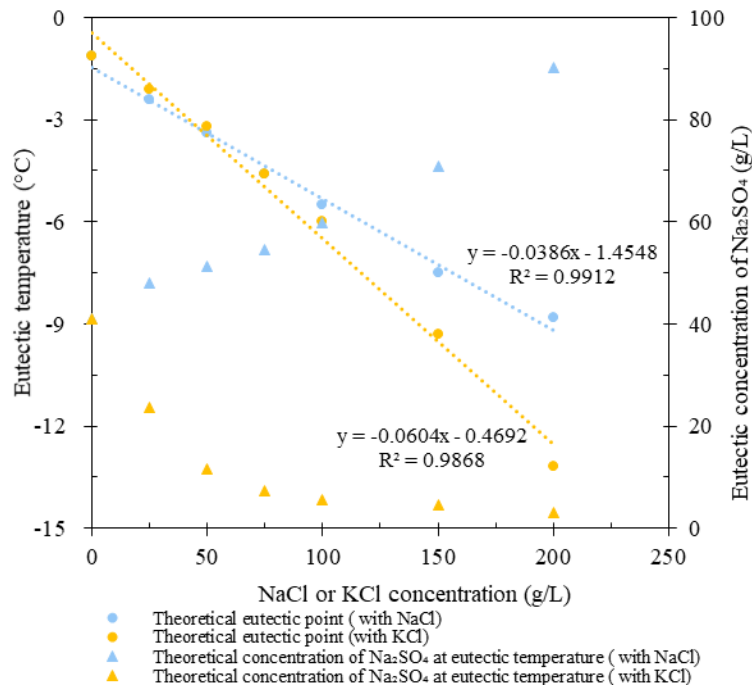


Figure 5.7 EP of Na₂SO₄ – H₂O system and eutectic concentration of Na₂SO₄ with different addition of KCl (0-150 g/L)

5.2 Scenario Study of using EFC to treat RO retentate

5.2.1 Effect of different Na₂SO₄ concentration in EFC

This simulation aims to investigate the relation between Na₂SO₄ and ice yield in a continuous mode of EFC. Due to the provided Na⁺ and SO₄²⁻ concentrations were far below the saturated concentration of Na₂SO₄ at 0°C, two smaller concentrations (2% and 3%) were selected. In this simulation, Na₂SO₄ was the only input solute. Each data point represents an equilibrium condition.

Figure 5.8 reflects the change in ice yield of 1 L solvent with decreasing temperature in the continuous EFC process. Each concentration profile could not reach 100% recovery. The higher concentration of Na₂SO₄ led to the later precipitation of ice and thus resulted in the variation of ice recovery. The ice yield had a largest jump at the EP. A highly concentrated solution induced a reduced ice yield at EP. There was a relatively large amount of ice needed to be moved before the temperature reached the EP (70%, 60% and 50% of total solvent with respect to 2 wt%, 3 wt%, 4 wt% Na₂SO₄). This result also reflected the relatively high yield of ice in one-stage EFC process.

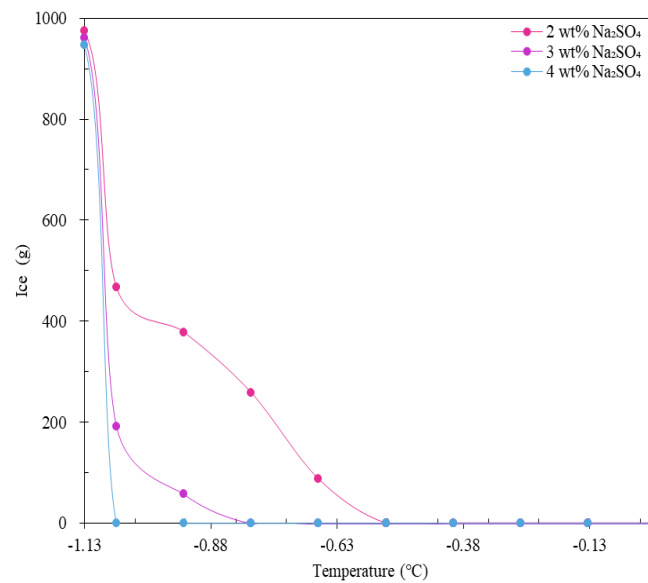


Figure 5.8 Effect of Na_2SO_4 concentration on ice recovery

Continuous EFC with 1 L of H_2O and three different concentrations (2 wt%, 3 wt%, 4 wt%) of NaCl as modelling input. The temperature ranged from 0 °C to the EP of the solution system.

5.2.2 Effect of NaCl concentration on the recovery of Na_2SO_4 and ice

Figure 6.9 compares the theoretical product yield of ice and salts in 1 L of H_2O in continuous EFC process of 4 wt% Na_2SO_4 when different NaCl was added. The solubility of NaCl is stable between 0 and 25°C³⁷. The different temperature ranges in figures were selected based on the EP of Na_2SO_4 - H_2O system. Table 5.1 gives the nucleation temperature of solid products predicted by OLI Stream Analyser. The recovery of H_2O and Na_2SO_4 before -21°C (formation temperature of $\text{NaCl}\cdot 2\text{H}_2\text{O}$) was calculated.

Table 5.1 Nucleation temperatures and solid recovery for solid compounds in continuous EFC of Na_2SO_4 (4 wt%) with different concentrations of NaCl

The inflow stream was 1 L of H_2O and ions with the concentrations shown in Table A4. The recovery was calculated based on mass.

	Nucleation temperature			
	No NaCl	50 g/L NaCl	100 g/L NaCl	150 g/L NaCl
Ice	-1.2 °C	-3 °C	-6 °C	-9 °C
$\text{Na}_2\text{SO}_4\cdot 10\text{H}_2\text{O}$	-1.2 °C	0 °C	0 °C	0 °C
$\text{NaCl}\cdot 2\text{H}_2\text{O}$	-	-21 °C	-21 °C	-21 °C
Ice recovery at -21°C	94.93%	78.13%	61.34%	44.54%
Na_2SO_4 recovery at -21°C	100%	99.32%	98.64%	97.96%

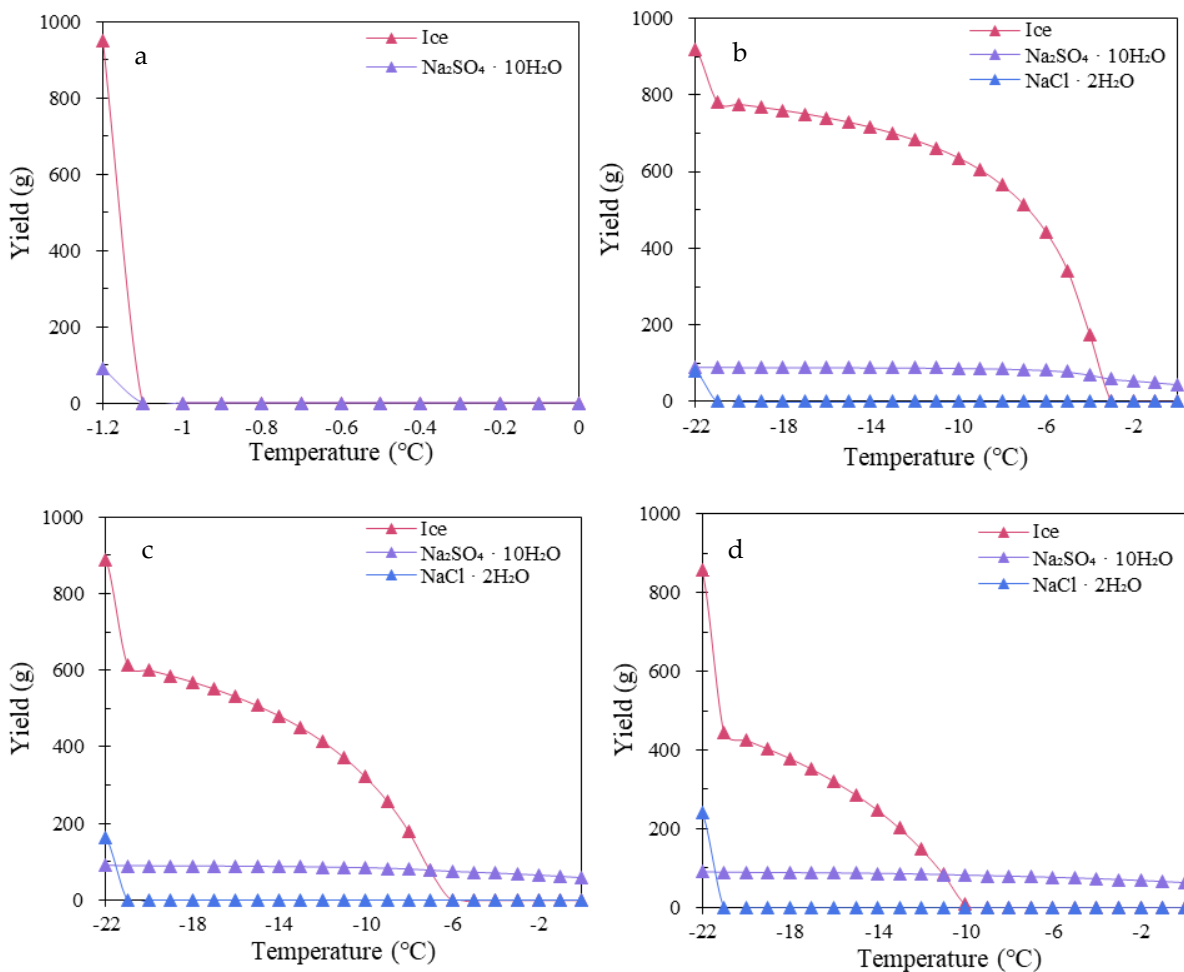


Figure 5.9 Solid yield at different NaCl concentrations in continuous EFC of Na_2SO_4

Inflow stream: 1 L H_2O , 4 wt% Na_2SO_4 and NaCl. (a) No NaCl, (b) 50 g/L NaCl, (c) 10 g/L NaCl, (d) 150 g/L NaCl.

According to the model, the mirabilite started to precipitate at about $-1.2\text{ }^\circ\text{C}$ in pure Na_2SO_4 aqueous solution. The ice reached a constant value quickly after that. Both solids became stable at $-3\text{ }^\circ\text{C}$. The theoretical recovery of ice and Na_2SO_4 reached 100% and 94.92% (mass-based).

Figure 5.10 presents the ice recovery with different addition of NaCl. Since the concentration of Na_2SO_4 in the solution was a bit higher than its solubility corresponded to the binary EP of $\text{Na}_2\text{SO}_4\text{-}10\text{H}_2\text{O}$ system, and the previous experiment showed that the existence of NaCl depresses the EP of Na_2SO_4 , it can be observed that mirabilite already precipitated at $0\text{ }^\circ\text{C}$. Ice started precipitating when the temperature reached the binary EP. The whole solution system reached a ternary EP when $\text{NaCl}\cdot 10\text{H}_2\text{O}$ formed at $-21\text{ }^\circ\text{C}$. Due to the precipitation of $\text{Na}_2\text{SO}_4\cdot 10\text{H}_2\text{O}$ and $\text{NaCl}\cdot 2\text{H}_2\text{O}$, the ice recovery at $-21\text{ }^\circ\text{C}$ decreased from 94.93% to 44.54% when NaCl concentration increased from 0 to 150 g/L. Figure 5.15 presents the $\text{Na}_2\text{SO}_4\cdot 10\text{H}_2\text{O}$ recovery with different addition of NaCl. It can be seen that the lines had two jumps when ice and $\text{NaCl}\cdot 2\text{H}_2\text{O}$ formed. The final theoretical Na_2SO_4 recovery can all reach 100%, so it was less affected by NaCl than ice.

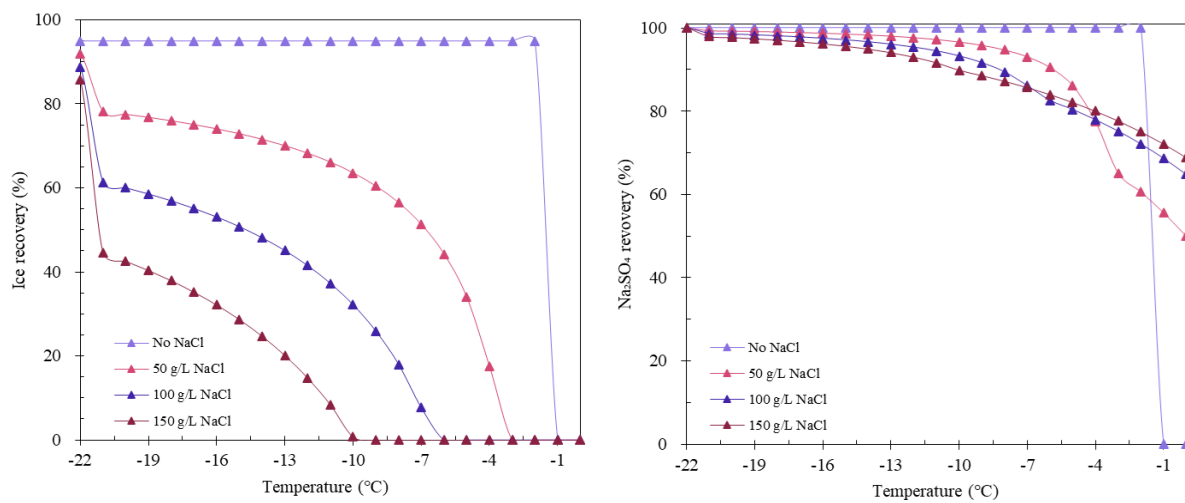


Figure 5.10 Ice and Na_2SO_4 recovery in the cooling process at different concentrations of NaCl
Inflow stream: 1 L H_2O , 4 wt% Na_2SO_4 and NaCl. The recovery was calculated based on mass.

Take 150 g/L NaCl concentration as an example. The mirabilite already started to precipitate at the beginning. Ice appeared at about -10°C with a recovery of 0.8 % at this moment. When temperature kept going down, $\text{NaCl}\cdot 2\text{H}_2\text{O}$ began to precipitate at -21°C , where both ice and $\text{Na}_2\text{SO}_4\cdot 10\text{H}_2\text{O}$ had a jump. After this jump, the ice recovery finally reached 85.67 % (mass-based 856.792 g). This value was lower than the ice recovery in pure Na_2SO_4 solution (100%), because there were $\text{NaCl}\cdot 2\text{H}_2\text{O}$ and $\text{Na}_2\text{SO}_4\cdot 10\text{H}_2\text{O}$ formed in the solution. So, if Na_2SO_4 is the only aimed salt to recover, the temperature should be controlled above the EP of $\text{NaCl}\cdot 2\text{H}_2\text{O}$ to prevent salt contamination. However, the recovery of H_2O at this temperature was less than 50%.

It can be observed that mirabilite precipitated in a larger recovery with increasing NaCl when the temperature was relatively high, but finally reached a lower yield at the EP of $\text{Na}_2\text{SO}_4\cdot 10\text{H}_2\text{O}$ system. However, the difference of mirabilite recovery between each concentration profile was less than ice recovery. Therefore, NaCl affects ice recovery more than salt mirabilite recovery.

5.2.3 Scenario 1: RO-NF-EFC

In this scenario, NF was the pre-treatment technology of RO retentate, NF concentrate played as the feed stream of continuous EFC process. From the brine information in Appendix C, Table A5, the dominant cations (Na^+ , K^+) and anions (SO_4^{2-} , Cl^-) provided the possible crystalline products.

Figure 5.11 presents the thermodynamic modelling results of this scenario. Four significant components precipitated out from NF concentrate, three were salts or salt hydrates, another one was ice. There were also other crystalline products such as CaCO_3 (Calcite), KCl (sylvite) and KNO_3 (Niter) but can be ignored regards their small portion. Each point represented an equilibrium condition. It can be observed that ice was the first crystallized compound and began to precipitate at -0.5°C . Its total recovery reached 86.5% at -2.25°C when $\text{Na}_2\text{SO}_4\cdot 10\text{H}_2\text{O}$

started precipitated (calculated based on the input ion data). $\text{Na}_2\text{SO}_4 \cdot 10\text{H}_2\text{O}$ (Mirabilite) was the first crystallized salt -2.25°C , followed by NaHCO_3 (Nahcolite) at -4.25°C , all of the four main crystalline products all precipitated out.

According to the simulation result, the recovery of Na_2SO_4 at -5°C was 84.114% with a yield of 2.21 g. The recovery of ice at -5°C was 95.803% with a yield of 958.03 g. These results reflected that EFC could reach a high recovery of ice and salt theoretically. As the aim of this treatment process was to effectively recover Na_2SO_4 and H_2O , though a high recovery was achieved, the low yield of Na_2SO_4 made it hard to be separated in the crystallizer. Apart from that, salt contamination may also happen if the temperature went down to -4.25°C . The process was ineffective in recovering salt as SO_4^{2-} concentration in the feed stream was not concentrated enough. Nevertheless, if the temperature can be controlled at -2°C where the H_2O recovery was 84.29%, this scenario can still reach an excellent separation of H_2O from the brine stream.

Table 5.2 Nucleation temperature of solid products in scenario 1

OLI simulation of a continuous EFC process. The inflow stream was with 1 L of H_2O and ions with the concentrations shown in Table A5. The recovery was calculated based on mass. The yield was converted from hydrate to the compound. OLI simulation of a continuous EFC process.

	Nucleation Temperature ($^\circ\text{C}$)	Mass-based recovery at -3°C (%)	Compound based yield (without H_2O) at -3°C (g)	Mass-based recovery at -5°C (%)	Compound based yield (without H_2O) at -5°C (g)
Ice	-0.5	90.437	904.37	95.803	958.08
$\text{Na}_2\text{SO}_4 \cdot 10\text{H}_2\text{O}$ (Mirabilite)	-2.25	37.422	1.96	84.114	2.21
NaHCO_3 (Nahcolite)	-4.25	-	-	49.560	1.50
$\text{NaCl} \cdot 2\text{H}_2\text{O}$ (Hydrohalite)	-22.25	-	-	-	-

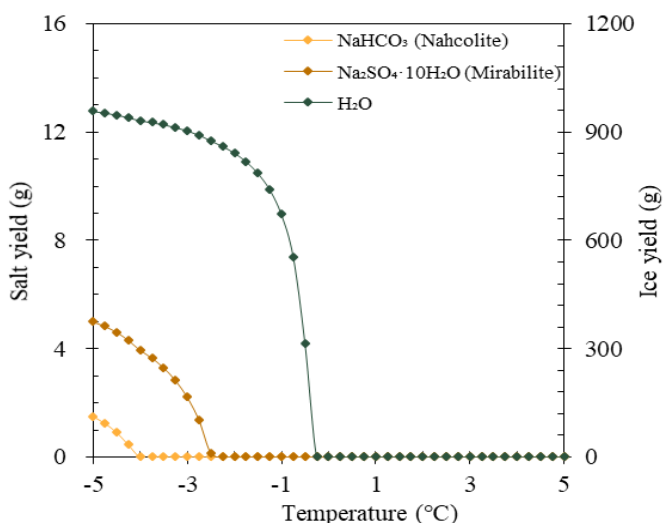


Figure 5.11 Product yields with temperature in scenario 1

As stated in the preliminary simulation result, directly recovering mirabilite at one-stage EFC crystallizer seemed impossible due to the low SO_4^{2-} concentration. One feasible method to

obtain more salt product was to place crystallizers in a series to concentrate the RO concentrate even further. Accordingly, a simulation to investigate the effect of enrichment times on the product yield was done.

The effect of the multi-stage continuous EFC process on the recovery of Na_2SO_4

In the multi-stage simulation, it was assumed that 60% of the formed ice is removed from the crystallizer with a 20% loss of Na_2SO_4 at each concentrate stage. This percentage was chosen based on the result stated in Chapter 4.3.1. Figure 5.12 shows the nucleation temperature of ice and mirabilite against the number of enrichment times. With more times of enrichment, the nucleation temperature of ice showed a downward tendency from -0.5°C to -4.25°C , while Na_2SO_4 formation temperature stayed the same (-4.25°C) until the fourth stage of concentrating. This finding revealed that in the first three stages of concentrating, the temperature profile of H_2O - Na_2SO_4 system followed all though the ice line shown in Figure 2.5. Then at the fourth stage, as concentrating caused Na_2SO_4 concentration continuously increased, the system crossed the ice line and got in touch with the salt line. Thus, the mirabilite appeared first at 5°C . The high concentration of mirabilite depressed the nucleation point of ice, which appeared until -4.25°C .

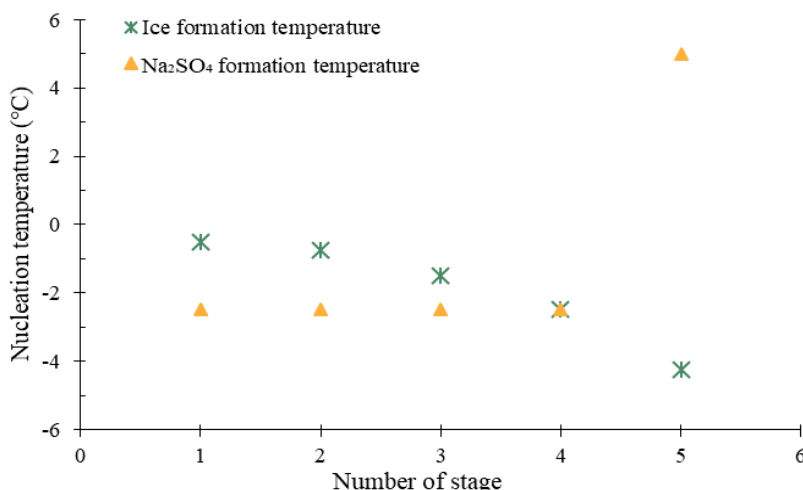


Figure 5.12 Nucleation temperature of ice and Na_2SO_4 at different number of concentrate times

In the EFC process, temperature control is a vital issue, because product yield as well as the purity are highly depending on the temperature. Even this thermodynamic model could not simulate the crystal properties. The solid composition and ion information under different temperature points give indications about the operation of EFC.

Two temperature points were chosen to investigate the influence of the number of the stage on product yield and composition. The first was -3°C . The ice formation point in four of the five simulations was -2.5°C , consider the existence of other ions (Mg^{2+} , Ca^{2+} , K^+ , etc.) could further depress the EP of H_2O - Na_2SO_4 system, -3°C was a relatively stable point. To make the analysis more comprehensive, -5°C was chosen as the second temperature. For one thing, it was still unknown to what extent the effect of accumulative NaHCO_3 and other ions on the depressing the temperature of the solution. From another, NaHCO_3 multiplied with

increasing enrichment times. With more enrichment time, the formation temperature of NaHCO_3 became earlier than ice (0°C in four-stage crystallization, ice formed at -4.25°C). It could be possible that the solution temperature dropped to this degree.

Figure 5.13 describes the effect of the number of the stage on the total solid mass and solid content proportion at -3°C . Theoretically, both ice and salt yield doubled when the number of stages was increased. It can be observed that at the same temperature, the mass of total solids reduced about 15% per stage. Among the three main solid products, ice was predominated in the first three enrichment simulations. The proportion of ice showed a downward trend, and this trend was accelerated. By contrast, the proportion and quality of salt products went up. At the fourth enrichment time, the high content of mirabilite became dominant, despite that the total mass of solids was comparatively low.

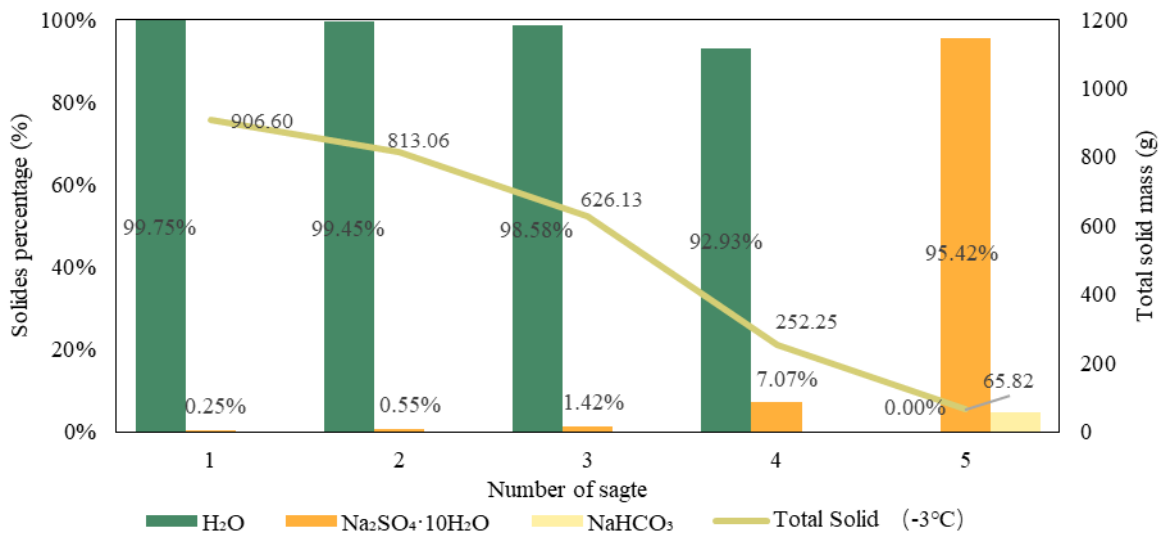


Figure 5.13 Solid content and total mass at different number of stage at -3°C in 1L of feed
At -3°C , there was not salt contamination, the solution system was relatively stable.

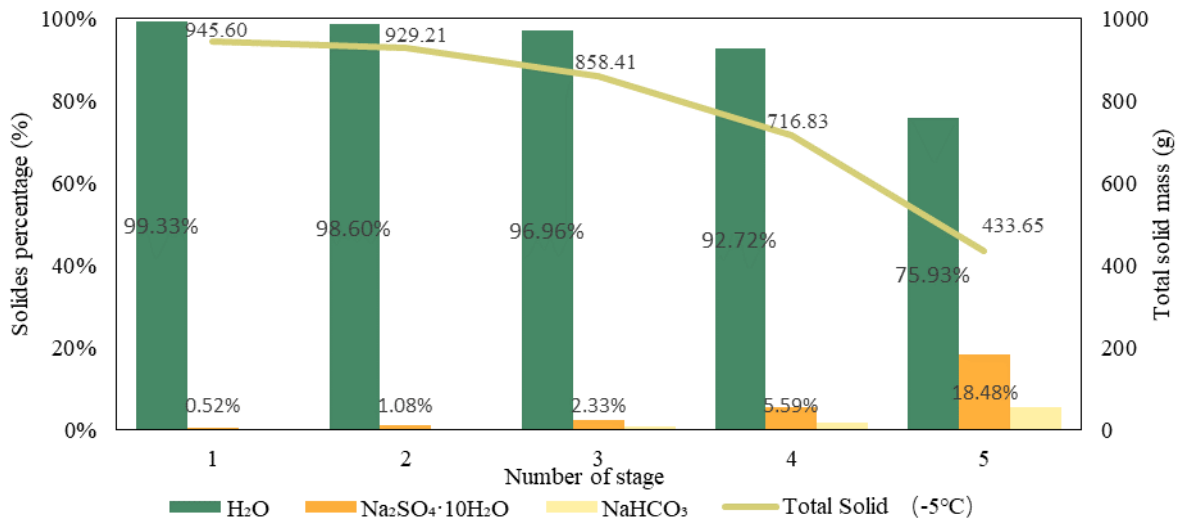


Figure 5.14 Solid composition and total mass at different number of stage at -5°C in 1L of feed

Figure 5.14 describes the effect of the number of the stages on the total solid mass and solid content proportion at -5°C . The overall trend was the same as depicted in Figure 5.13, but the

total solid level was higher than it was at -3°C . The product content of each compound did not change a lot, except about 24.3 g of NaHCO_3 precipitated and caused salt contaminant at a five-stage crystallization.

The problem in this scenario is tricky. From one thing, one-stage crystallization process resulted in a less salt product. However, the gap between the nucleation temperatures of ice and mirabilite was suitable for only recovering H_2O . From another, the multi-stage operations made the product yield increase. However, the nucleation temperature of ice and mirabilite became closer. Although the multi-stage operation promoted the formation of mirabilite, it was still unable to make up for the considerable gap between the ice and mirabilite yield, and it may inhibit the separation performance.

5.2.4 Scenario 2: RO-TOC-NF-EFC

Compare with the brine of Scenario 1: RO-NF-EFC, the brine of Scenario 2 contained double times of Na^+ , the SO_4^{2-} concentration was about ten times as it in Scenario 1: RO-NF-EFC, the HCO_3^- and Cl^- concentration were obviously less. Moreover, more metal compounds were presented in the brine.

Table 5.3 lists the nucleation temperature of the solid products and corresponding recovery. Both ice and $\text{Na}_2\text{SO}_4 \cdot 10\text{H}_2\text{O}$ had a comparatively high recovery. Ice precipitated at -0.75°C , which was lower than the ice nucleation temperature in 4 wt% Na_2SO_4 solution in Chapter 5.2.2, Figure 5.8. It means that the concentration of Na_2SO_4 in the stream of scenario 2 was a bit lower than 4 wt%. The nucleation temperature of mirabilite was -1.25°C , which was almost the same as the one in Chapter 5.2.2, Figure 5.8. Therefore, the effect of the small portion of Cl^- on the precipitation temperature of the solid product could be neglected. The double salt $\text{K}_2\text{SO}_4 \cdot \text{CaSO}_4 \cdot \text{H}_2\text{O}$ (Syngenite) crystallized at -3.75°C but only in a tiny portion, so its effect can be ignored.

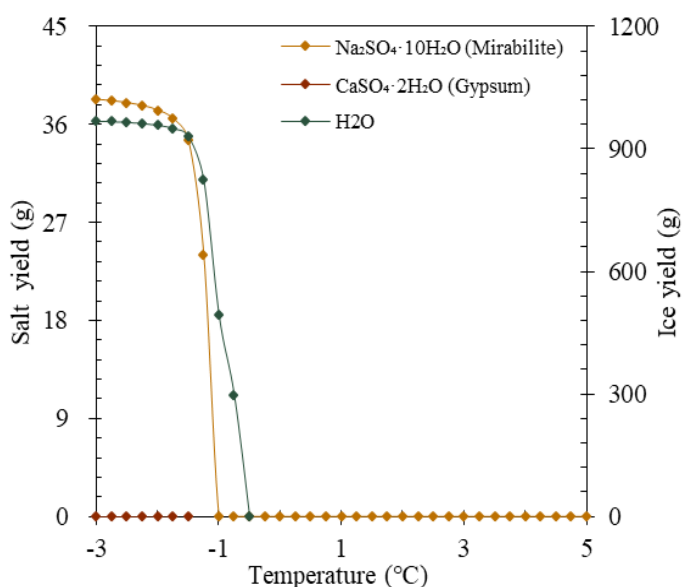
Compare with the nucleation temperatures of the solids product in Scenario 1: RO-NF-EFC, the nucleation temperature of the ice in this scenario was lower while the one of mirabilite was higher. This phenomenon indicated that SO_4^{2-} in this scenario was more concentrated than Scenario 1. Besides, there may be a relation that high concentration level of Na^+ led to a high crystallization temperature for $\text{Na}_2\text{SO}_4 \cdot 10\text{H}_2\text{O}$. This phenomenon was the same as the finding of Randall et al. ⁹.

In Figure 6.19, the product yields with temperature were graphically depicted. Two main solid products were ice and mirabilite. $\text{CaSO}_4 \cdot 2\text{H}_2\text{O}$ (Gypsum) and KNO_3 (Niter) presented with low yields so can be ignored. The TOC removal unit introduced extra SO_4^{2-} , the mirabilite yield was far more than it was in Scenario 1: RO-NF-EFC. Nonetheless, it still had potential been hidden by ice in terms of their huge yield gap. Another point was that the nucleation point of ice and mirabilite was close, which makes it hard to control the temperature and to precipitate ice solely.

Table 5.3 Nucleation temperature of solid products in scenario 2

OLI simulation of a continuous EFC process. The inflow stream was 1 L of H₂O and ions with the concentrations shown in Table A6. The recovery was calculated based on mass. The yield was converted from hydrate to the compound.

	Nucleation Temperature (°C)	Mass-based recovery at -3°C (%)	Compound based yield (without H ₂ O) at -3°C (g)
Ice	-0.75	96.926	969.26
Na ₂ SO ₄ ·10H ₂ O (Mirabilite)	-1.25	98.380	16.88
CaSO ₄ ·2H ₂ O (Gypsum)	-1.5	94.926	0.0067
K ₂ SO ₄ ·CaSO ₄ ·H ₂ O (Syngenite)	-3.75	0	0
KNO ₃ (Niter)	-9.5	0	0
NaCl·2H ₂ O (Hydrohalite)	-25	0	0

**Figure 5.15 Product yields with temperature in scenario 2**

5.2.5 Scenario 3: RO-TOC-EFC

In this scenario, instead of going to the NF, the effluent from the TOC removal unit was directly transported to EFC unit. Without any pre-concentration step, the stream contained the least Na⁺ and SO₄²⁻ out of the four scenarios; the other concentrations of ions were little as well. Therefore, it was expected to have a higher precipitation point of ice due to a weaker common ion effect and salt effect. The simulation results confirmed this hypothesis.

Table 6.4 shows the nucleation points of the solids compound. Ice formed at -0.25°C. The precipitation point of mirabilite was -1.25°C. Those were close to the one in pure 4 wt% Na₂SO₄ solution in Chapter 5.2.2. Ca₅(OH)(PO₄)₃ (Hydroxylapatite) was an uncommon electrolyte formed at an early stage, but its small quality did not affect the EP of Na₂SO₄- H₂O system according to the simulation result.

Figure 5.16 presents the product yield of this scenario. The lower salt concentrations led to a high recovery of ice as less hydrate formed. It can be calculated that the theoretical recovery of ice and mirabilite at -3°C reached 99.158% and 96.417%, respectively. The yields of them were 99.158 g and 2.910 g (with $\text{Na}_2\text{SO}_4 \cdot 10\text{H}_2\text{O}$ 6.598 g). Theoretically, due to the effect of other ions effects such as K^+ , Mg^{2+} , and Cl^- , the temperature in the reactor would slowly decrease until the last solid compound precipitated out. During the meanwhile, the recovery of solids products increases. However, these implications are negligible if those ions are with low concentration in reality.

The optimal function of EFC in this scenario was to recover water. Controlling the temperature between -0.25 to -1.25°C so that the high yield of ice can be separated from the crystallizer. The interference of HOC_3^- was less and more significant yield of mirabilite than Scenario 1: RO-NF-EFC.

Table 5.4 Nucleation temperature of solid products in scenario 3

OLI simulation of a continuous EFC process. The inflow stream was 1 L of H_2O and ions with the concentrations shown in Table A7. The recovery was calculated based on mass. The yield was converted from hydrate to the compound.

	Nucleation Temperature ($^{\circ}\text{C}$)	Mass-based recovery at -3°C (%)	Compound based yield (without H_2O) at -3°C (g)
Ice	-0.25	99.158	991.58
$\text{Na}_2\text{SO}_4 \cdot 10\text{H}_2\text{O}$ (Mirabilite)	-1.25	96.417	2.910
$\text{Ca}_5(\text{OH})(\text{PO}_4)_3$ (Hydroxylapatite)	5	100.000	0.0008

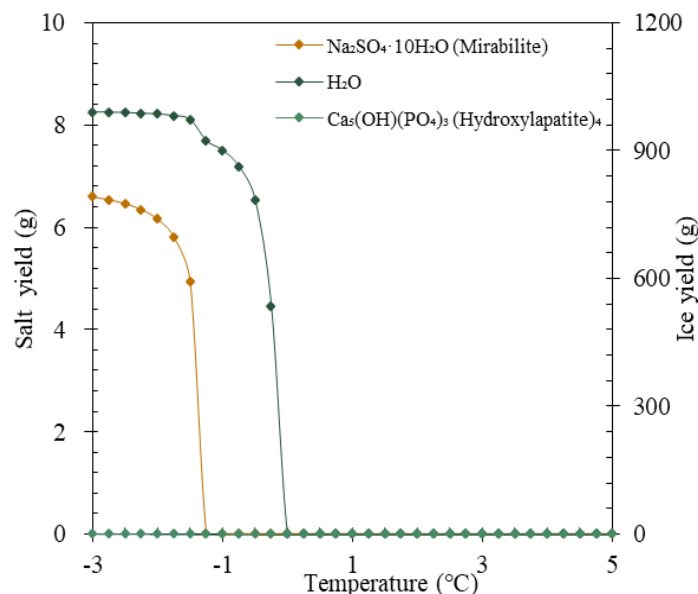


Figure 5.16 Product yields with temperature in scenario 3

5.2.6 Scenario 4: RO-TOC-NF-RO-EFC

In this scenario, the pre-treatment steps of DWP RO retentate included TOC, NF, RO. NF rejection was treated by RO, then RO retentate was the feed of EFC. Due to the limited ion

concentration data, WAVE[®] was applied to predict the RO concentrate after NF. It was assumed that the last RO had 75% of TOC removal rate and 70% of water recovery. The SI of RO retentate was 0.169, so there was not scaling tendency. This RO concentrated the main ions in the NF rejection significantly. The feed stream of EFC contained an extremely high concentration of Na⁺ and SO₄²⁻.

Table 5.5 displays the nucleation temperature, mass-based recovery and yield of crystalline product at -3°C. Na₂SO₄ reached its solubility limitation before 0°C. Ice crystal began to form at -1.25°C. The water recovery was 92.108%, which was the lowest among the four scenarios. With 102.408 g yield of mirabilite, the Na₂SO₄ recovery reached 98.490%, which was the biggest among the four scenarios.

As indicated in Figure 5.17, the gap of nucleation temperature between ice and mirabilite was large. From this point of view, it seemed to be capable of retrieving Na₂SO₄ from waste brine before ice crystal forms and achieving a sequential recover of Na₂SO₄ and freshwater. However, according to the result of WAVE[®], the RO permeate contained large amount of SO₄²⁻, Na⁺ and NO₃⁻, which led to another brine stream. The treatment efficiency of this RO was insufficient.

Actually, if taking the design information of WAVE[®] into consideration, the RO was impossible to achieve the high recovery and high quality of permeate at the same time. With several tries, it was found that with a high quality of permeate the excess of SO₄²⁻ and Ca²⁺ in RO retentate resulted in severe scaling of RO membrane. While reducing the scaling tendency of RO retentate led to poor quality of permeate. If so, the design of this scenario goes against the concept of ZLD and cause extra burden to the facilities. Therefore, this scenario was not practical for either recovering H₂O or Na₂SO₄. But this was concluded based on insufficient information and assumptions. With more detailed information from the RO unit, the more accurate predictions can be made for this scenario.

Table 5.5 Nucleation temperature of solid products in scenario 4

OLI simulation of a continuous EFC process. The inflow stream was 1 L of H₂O and ions with the concentrations shown in Table A8. The recovery was calculated based on mass. The yield was converted from hydrate to the compound.

	Nucleation Temperature (°C)	Mass-based recovery at -3°C (%)	Compound based yield (without H ₂ O) at -3°C (g)
Na ₂ SO ₄ ·10H ₂ O (Mirabilite)	0.25	98.490	45.161
Ice	-1.25	92.108	921.078
CaSO ₄ ·2H ₂ O (Gypsum)	-1.5	96.095	0.
K ₂ SO ₄ ·CaSO ₄ ·H ₂ O (Syngenite)	-3.25	0	0

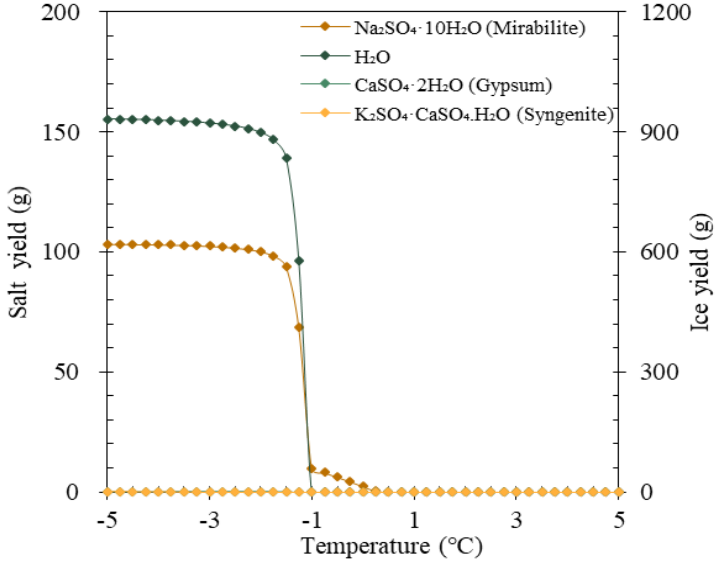


Figure 5.17 Product yields with temperature in scenario 4

Chapter 6 Conclusions

This study has determined the phase diagram of Na_2SO_4 - H_2O binary system with different concentrations of NaCl by running crystallization experiments. A thermodynamic model in OLI Analyser was used in parallel to compare with the experimental results. A scenario study was conducted to find an optimal process to recover Na_2SO_4 and H_2O . According to the conducted experiments and simulation, the listed research questions can be answered:

(1) The solubility and eutectic concentration of Na_2SO_4 will increase or decrease with increasing NaCl concentrations?

The presence of NaCl decreased the solubility of Na_2SO_4 due to the common ion effect, but the decreasing tendency was decelerated with increasing NaCl. The experimental results of solubility had a high-degree coincidence with the simulation results. The effect of KCl was further compared with NaCl in the model. In contrast, KCl promoted the dissolution of Na_2SO_4 , and it can be explained by the salting-in effect between the two salts.

(2) Will the EP of Na_2SO_4 - H_2O system decrease with increasing NaCl concentration?

The rising level of NaCl depressed the EP of Na_2SO_4 - H_2O binary system. The decreased EP showed a linear trend. The model showed that the change of EP had better accuracy with theoretical value than the change of eutectic concentration of Na_2SO_4 .

(3) How much the ice and Na_2SO_4 recovery in EFC would be with the different pre-treatment process?

All of the four scenarios achieved more than 92% of ice recovery. Except Scenario 1 (84.4%), the rest of the three scenarios reached more than 96% of Na_2SO_4 recovery at -3°C .

Though the theoretical recovery of Na_2SO_4 and H_2O were high, the goal of recovering Na_2SO_4 was hard to accomplish. The ice yield was far in excess of the mirabilite in all of the scenarios. A pre-concentration step is needed to recover Na_2SO_4 . The result from Scenario 1 reflected that the pre-concentration stage in diluted solution led to a closer nucleation temperature of ice and mirabilite, which may bring difficulties for separation work. In Scenario 2, the closer nucleation temperature of ice and mirabilite was more prone to cause a mixture. Scenario 3 was too diluted to harvest Na_2SO_4 . Scenario 4 was most likely to accomplish the highest recovery of Na_2SO_4 . However, the RO unit in this scenario causes low H_2O recovery, poor quality of permeate and scaling issue, which could not be tackled at the same time.

The result also indicated that the optimal temperature range to operate the crystallizer was between -1.25°C to -3°C . Both Scenario 1 and Scenario 3 can be considered as feasible processes to recover only H_2O if the temperature can be controlled well.

In conclusion, EFC brings us closer to the sustainable ZLD concept. It is an effective tool to recover H_2O from industrial RO retentate. The presence of NaCl is a double-edged sword. It enlarges the gap of the nucleation temperatures but may cause less purity, which needs further vilification through experiment. The impurity study of EFC is still underway. The recovery of H_2O and salt are highly depending on the composition of feed stream. It is recommended to study the combined effect of the ions in the waste stream since they have a synergistic or compensatory effect.

Chapter 7 Research limitations and recommendations

Based on the conducted experiments and the thermodynamic model, several limitations of this research are stated below. Besides, the corresponding suggestions are given to improve the current methodology and future research. The original objective of this work was to investigate how the different concentrations of NaCl or humic acid affect the crystallization kinetics and the quality of solid products in EFC of Na₂SO₄. As a result of COVID-19, the experiment did not go as planned. Only the study about the effect of NaCl on the solubility of Na₂SO₄ was processed in the laboratory.

7.1 The experiment set up and design

Ice scaling phenomenon was severe. The smooth inner wall provided ideal attachment points. Gradually, the rapid increase of ice layer thickness retarded the rotation of scraper. Therefore, improving the design of scraper is in urgent need.

In response to the problem of mixing solid liquids occurred when using a syringe to take the liquid sample, it would be better to create a low-temperature environment for the operation of sampling and filtration or finding a more effective way to filtrate the solids. Otherwise, the quickly melt solids in the syringe add more error to the experiment.

Improve ion analysis techniques. An accurate ion analysis makes the calculation of solubility more precise, and the ion data as the input in the thermodynamic model could be more convinced. A consistent analysis makes the results more reliable, especially when more dilution times are needed.

The partial solubility experiment of the salt line was conducted without seeding. It is also recommended that run the partial experiment of salt line with seeding to see if the nucleation temperature of ice changes. Combine the temperature profile with the phenomenon in the crystallizer for a better observation.

For further exploration, the following research questions are still worthy of answering:

- (1) How will the different concentrations of NaCl affect the crystallization kinetics and the quality of ice and Na₂SO₄ and ice in EFC?

- How are the crystallization kinetics (nucleation rate growth rate) of ice and Na_2SO_4 are altered by different NaCl concentrations?
- How are the morphology and size of ice and salt crystals changed by different NaCl concentrations in EFC?
- How does the different NaCl concentrations affect the ice purity in EFC ?
- Does the fast cooling cause different effect on crystallization behaviour by different NaCl concentrations in EFC?

(2) How will the presence of humic acid affect the crystallization kinetics and the quality of ice and Na_2SO_4 and ice in EFC?

- Does the presence of humic acid increase or decrease the ice and mirabilite yield of sodium sulfate salt in EFC?
- How do the morphology and crystal size changed by different humic acid concentrations in EFC?
- Does the presence of humic acid increase or decrease the ice crystal purification efficiency in EFC?
- Do the impurities physically adhere on the ice surface or incorporated into the Na_2SO_4 crystal lattice?

7.2 Modelling study about continuous EFC

All of the simulation results should be experimentally verified or being evaluated with related experimental results. The analysis should be combined with crystallization kinetics such as morphology and crystal size distribution. The kinetics of the system should also be taken into account. For example, the incubating time and energy consumption and economy. It is recommended to further explore in terms of those aspects.

In Scenario 1: RO-NF-EFC, the existence of NaHCO_3 was found. Whether the same concentration of NaHCO_3 in the feed will depress EP, and to what extent it will are uncertain. The relevant experiment can be conducted to explore that. The feed stream of Scenario 2: RO-TOC-NF-EFC and Scenario 3:RO-TOC-EFC were both diluted. A further simulation that investigates the influence of enrichment on these two scenarios can be attempted. Moreover, in Scenario 2: RO-TOC-NF-EFC, which is the most used routine at present, the results showed that salt contamination might happen in a significant probability. It can be overcome by testing the kinetics of the crystallization.

The study on the effect of organic matter in the EFC process needs to be prompted, some qualitative research has been done, but the quantitative analysis is insufficient. Besides, the process conditions, detailed ion information and process regulations of each treatment unit were not clear. More additional measurements of the process would provide more accurate indications.

References

1. UNESCO. *The United Nations World Water Development Report 2018: Nature-Based Solutions for Water*. (WWAP (United Nations World Water Assessment Programme)/UN-Water, 2018).
2. WHAT IS ZERO BRINE - ZERO BRINE. <https://zerobrine.eu/about-us/> (2020).
3. Hubbe, M., Mayer, E., Becheleni, A., Lewis, A. & Shi, S. Q. *Recovery of Inorganic Compounds from Spent Alkaline Pulping Liquor by Eutectic Freeze Crystallization and Supporting Unit Operations: A Review*. <https://www.researchgate.net/publication/328075584>.
4. Nathoo, J., Jivanji, R. & Lewis, A. E. *FREEZING YOUR BRINES OFF: EUTECTIC FREEZE CRYSTALLIZATION FOR BRINE TREATMENT*.
5. Van Der Ham, F., Witkamp, G. J. J., de Graauw, J. & van Rosmalen, G. M. M. Eutectic freeze crystallization: Application to process streams and waste water purification. *Chem. Eng. Process. Process Intensif.* **37**, 207–213 (1998).
6. Randall, D. G., Nathoo, J. & Lewis, A. E. A case study for treating a reverse osmosis brine using Eutectic Freeze Crystallization-Approaching a zero waste process. *Desalination* **266**, 256–262 (2011).
7. Reddy, S. T., Lewis, A. E., Witkamp, G. J., Kramer, H. J. M. & van Spronsen, J. Recovery of Na₂SO₄·10H₂O from a reverse osmosis retentate by eutectic freeze crystallisation technology. *Chem. Eng. Res. Des.* **88**, 1153–1157 (2010).
8. Peters, E. M., Chivavava, J., Rodriguez-Pascual, M. & Lewis, A. E. Effect of a Phosphonate Antiscalant during Eutectic Freeze Crystallization of a Sodium Sulfate Aqueous Stream. *Ind. Eng. Chem. Res.* **55**, 9378–9386 (2016).
9. Randall, D. G. Development of a brine treatment protocol using Eutectic Freeze Crystallization Diss. University of Cape Town (2010).
10. Crafts, P. Chapter 2 - The Role of Solubility Modeling and Crystallization in the Design of Active Pharmaceutical Ingredients. in *Chemical Product Design: Toward a Perspective Through Case Studies* (eds. Ng, K. M., Gani, R. & Dam-Johansen, K. B. T.-C. A. C. E.) vol. 23 23–85 (Elsevier, 2007).
11. Beckmann, W. *Crystallization: Basic Concepts and Industrial Applications*. *Crystallization: Basic Concepts and Industrial Applications* (Wiley-VCH, 2013). doi:10.1002/9783527650323.
12. Allan S Myerson. *Handbook of industrial crystallization*, Butterworth-Heinemann. (2002).
13. Sugimoto, T. & Sugimoto, T. NUCLEATION. *Monodispersed Part*. 1–85 (2001) doi:10.1016/B978-044489569-1/50019-1.
14. Scherer, G. W. Crystallization in pores. *Cem. Concr. Res.* **29**, 1347–1358 (1999).
15. Byrappa, B. 2.1.1 Driving Force. in *Crystal Growth Technology* (William Andrew Publishing/Noyes, 2003).

16. Misra, P. K. & Misra, P. K. Basic Properties of Crystals. *Phys. Condens. Matter* 1–35 (2012) doi:10.1016/B978-0-12-384954-0.00001-3.
17. Lee, K. Y. Model to Describe the Binodal Curve on a Type 1 Ternary Phase Diagram. *J. Environ. Eng.* **136**, 650–656 (2010).
18. Salvador Cob, S., Genceli Güner, F. E., Hofs, B., van Spronsen, J. & Witkamp, G. J. Three strategies to treat reverse osmosis brine and cation exchange spent regenerant to increase system recovery. *Desalination* **344**, 36–47 (2014).
19. Fernández-Torres, M., Ruiz-Beviá, F., Rodríguez-Pascual, M. & von Blottnitz, H. Teaching a new technology, eutectic freeze crystallization, by means of a solved problem. (2012) doi:10.1016/j.ece.2012.07.002.
20. Eutectic Freeze Crystallization | Cool Separations. <https://www.coolseparations.nl/efc-technology-how-it-works/>.
21. Lu, X. Novel Applications of Eutectic Freeze Crystallization. (Technische Universiteit Delft, 2014).
22. Heydenrych, H., Pascual, M. R. & Lewis, A. *Continuous Eutectic Freeze Crystallization*. (2018).
23. Lin, C. Y. & Pan, J. Y. The effects of sodium sulfate on the emissions characteristics of an emulsified marine diesel oil-fired furnace. *Ocean Eng.* **28**, 347–360 (2001).
24. Randall, D. G., Zinn, C. & Lewis, A. E. Treatment of textile wastewaters using Eutectic Freeze Crystallization. (2014) doi:10.2166/wst.2014.289.
25. Becheleni, E. M. A., Rodriguez-Pascual, M., Lewis, A. E. & Rocha, S. D. F. Influence of Phenol on the Crystallization Kinetics and Quality of Ice and Sodium Sulfate Decahydrate during Eutectic Freeze Crystallization. *Ind. Eng. Chem. Res.* **56**, 11926–11935 (2017).
26. Hasan, M., Rotich, N., John, M. & Louhi-Kultanen, M. Salt recovery from wastewater by air-cooled eutectic freeze crystallization. *Chem. Eng. J.* **326**, 192–200 (2017).
27. Jooste, Debora. Ice scaling in continuous eutectic freeze crystallization. Diss. University of Cape Town (2016).
28. John, M. *et al.* Impurity separation efficiency of multi-component wastewater in a pilot-scale freeze crystallizer. *Sep. Purif. Technol.* 116271 (2019) doi:10.1016/j.seppur.2019.116271.
29. Vaessen, R., Seckler, M. & Witkamp, G. J. Eutectic freeze crystallization with an aqueous KNO₃-HNO₃ solution in a 100-L cooled-disk column crystallizer. *Ind. Eng. Chem. Res.* **42**, 4874–4880 (2003).
30. Lewis, A. E. *et al.* Design of a Eutectic Freeze Crystallization process for multicomponent waste water stream. *Chem. Eng. Res. Des.* **88**, 1290–1296 (2010).
31. Leyland, D., Chivavava, J. & Lewis, A. E. Investigations into ice scaling during eutectic freeze crystallization of brine streams at low scraper speeds and high supersaturation. *Sep. Purif. Technol.* **220**, 33–41 (2019).
32. Chen, P. *et al.* Recovering sodium erythorbate from wastewater through freeze crystallization technology. *Water Environ. Res.* **91**, 455–461 (2019).
33. Lorenz, H. & Beckmann, W. Purification by Crystallization. *Crystallization* 129–148 (2013) doi:doi:10.1002/9783527650323.ch7.
34. Pronk, P., Ferreira, C. A. I., Pascual, M. R. & Witkamp, G. J. Maximum temperature difference without ice-scaling in scraped surface crystallizers during eutectic freeze crystallization. *VDI Berichte* 1141–1146 (2005).

35. Wang, P., Anderko, A. & Young, R. D. A speciation-based model for mixed-solvent electrolyte systems. *Fluid Phase Equilib.* **203**, 141–176 (2002).
36. National Center for Biotechnology Information. PubChem Database. Sodium chloride, CID=5234. <https://pubchem.ncbi.nlm.nih.gov/compound/Sodium-chloride>.
37. Farnam, Y., Bentz, D., Sakulich, A., Flynn, D. & Weiss, J. Measuring Freeze and Thaw Damage in Mortars Containing Deicing Salt Using a Low-Temperature Longitudinal Guarded Comparative Calorimeter and Acoustic Emission. *Adv. Civ. Eng. Mater.* **3**, 20130095 (2014).

Appendix

Appendix A: Experiment set-up



Figure A1 Crystallizer for the batch experiment



Figure A2 Consort C3010 multi-parameter analyser



Figure A3 Lauda RP4080 CW thermal controller

Appendix B: Thermodynamic model input of OLI Analyser

Table A1 Model input: effect of NaCl concentrations on the solubility of Na₂SO₄

	NaCl concentration (g/L)				
	0	50	100	150	200
H ₂ O (g)	1000	1000	1000	1000	1000
Na ₂ SO ₄ (g)	-	-	-	-	-
NaCl (g)	0	50	100	150	150

Table A2 Model input: effect of KCl concentrations on the solubility of Na₂SO₄

	KCl concentration (g/L)				
	0	50	100	150	200
H ₂ O (g)	1000	1000	1000	1000	1000
Na ₂ SO ₄ (g)	-	-	-	-	-
KCl (g)	0	50	100	150	150

Table A3 Model input: the ice yield at different Na₂SO₄ concentrations

	Na ₂ SO ₄ concentration		
	1 wt%	2 wt%	3 wt%
H ₂ O (g)	1000	1000	1000
Na ₂ SO ₄ (g)	10.10	20.41	30.93

Table A4 Model input of the simulation about the effect of NaCl on the recovery of mirabilite

	NaCl concentration (g/L)				
	0	50	100	150	200
H ₂ O (g)	1000	1000	1000	1000	1000
Na ₂ SO ₄ (g)	40	40	40	40	40
NaCl (g)	0	50	100	150	200
Temperature (°C)	0 ~ -30	0 ~ -30	0 ~ -30	0 ~ -30	0 ~ -30

Appendix

Table A5 Ion concentration of NF concentrate, scenario 1

Temperature (°C)	25
Conductivity (mS/cm)	8.2
pH	9.1
	Concentration (mg/L)
NH ₄ ⁺	<1
K ⁺	58
Na ⁺	2300
Ca ²⁺	<4
Mg ²⁺	<2.5
NO ₃ ⁻	12
Cl ⁻	1329
SO ₄ ²⁻	1173
HCO ₃ ⁻	2214
PO ₄ ³⁻	<5
Fe	0.054
Mn	<0.0055
Zn	0.015
B	0.027
Cu	0.184
Mo	0.116
TOC	45.32

Appendix

Table A6 Ion concentration of NF concentrate after TOC removal unit, scenario 2

Temperature (°C)	25
Conductivity (mS/cm)	18
pH	3
	Concentration (mg/L)
NH ₄ ⁺	<1
K ⁺	89
Na ⁺	5304
Ca ²⁺	31
Mg ²⁺	3.9
Si	115
NO ₃ ⁻	182
Cl ⁻	132
SO ₄ ²⁻	11651
HCO ₃ ⁻	<6
PO ₄ ³⁻	8.8
Fe	5.673
Mn	0.257
Zn	3.595
B	0.223
Cu	1.655
TOC	16.2
Total cation (meq/L)	234.85
Total inion (meq/L)	249.5
Imbalance (meq/L)	14.65

Appendix

Table A7 Ion concentration in effluent of TOC removal unit, scenario 3

Temperature (°C)	25
Conductivity (mS/cm)	4.8
pH	3
	Concentration (mg/L)
NH ₄ ⁺	<1
K ⁺	16
Na ⁺	964
Ca ²⁺	4.4
Mg ²⁺	<2.5
Si	18.3
NO ₃ ⁻	109
Cl ⁻	76
SO ₄ ²⁻	2041
HCO ₃ ⁻	<6
PO ₄ ³⁻	<5
Fe	0.374
Mn	0.036
Zn	0.078
B	0.089
Cu	0.075
TOC	4.2
Total cation (meq/L)	42.7
Total inion (meq/L)	46.6
Imbalance (meq/L)	3.88

Table A8 Ion concentration in the last RO retentate, scenario 4

	Concentration (mg/L)
Temperature (°C)	25
Conductivity (mS/cm)	4.8
pH	2.7
NH ₄ ⁺	2.55
K ⁺	226.4
Na ⁺	15000
Ca ²⁺	94.67
Mg ²⁺	9.99
Si	-
NO ₃ ⁻	332.6
Cl ⁻	286.9
SO ₄ ²⁻	31078
HCO ₃ ⁻	-
PO ₄ ³⁻	-
Fe	-
Mn	-
Zn	-
B	-
Cu	-
TOC	-
Total cation (meq/L)	663.4
Total inion (meq/L)	660.9
Imbalance (meq/L)	2.5

Saturation state calculation:

(1) Ionic strength:

$$I = \frac{1}{2} \sum m_i z_i^2$$

Where z is the electric charge of the ith ion, m is ion concentration

(2) Calculation of activity coefficient:

$$\log \gamma_i = -Az_i^2 \left(\frac{\sqrt{I}}{1 + \sqrt{I}} - 0.3I \right)$$

where A is ion-specific parameters, in this case $A = 0.5085$

(3) Saturation index:

$$SI = \log \left(\frac{IAP}{K} \right)$$

$$IAP_{gypsum} = [Ca^{2+}][SO_4^{2-}]$$

Where K is the solubility product equilibrium constant. In this case $K_{gypsum} = 4.93 \times 10^{-5}$

Appendix C: Fitting curves and K_{sp} values

Table A9 Fitting functions, solubility calculation results, ion concentrations and K_{sp} of Na_2SO_4 at 0°C when NaCl concentration changes

T= 0°C	Logarithmic distribution function	Solubility (%)	Na_2SO_4 (g/L)	SO_4^{2-} (mol/L)	Na^+ (mol/L)	K_{sp}
25 g/L NaCl	$y = -23.5 + 16\ln(x + 1.862)$	2.48180199	25.44962934	0.17922274	0.35844548	0.02302711
50 g/L NaCl	$y = -6.50314 + 10\ln(x + 0.05957)$	1.9101854	19.47384049	0.13713972	0.27427944	0.01031691
75 g/L NaCl	$y = -2.84106 + 9.47894\ln(x - 0.15982)$	1.50930547	15.3243459	0.10791793	0.21583586	0.00502737
100 g/L NaCl	$y = -1.48123 + 9.14998\ln(x - 0.23662)$	1.41234316	14.3257605	0.10088564	0.20177127	0.00410722
150 g/L NaCl	$y = -2.25513 + 9.87099\ln(x - 0.23692)$	1.49328372	15.15920716	0.10675498	0.21350996	0.00486659
200 g/L NaCl	$y = -0.45 + 9.34\ln(x - 0.32)$	1.36935939	13.88371179	0.09777262	0.19554524	0.00373862

Table A10 Fitting functions, solubility calculation results, ion concentrations and K_{sp} of Na_2SO_4 at 5°C when NaCl concentration changes

T= 5°C	Logarithmic distribution function	Solubility (%)	Na_2SO_4 (g/L)	SO_4^{2-} (mol/L)	Na^+ (mol/L)	K_{sp}
25 g/L NaCl	$y = -23.5 + 16\ln(x + 1.862)$	4.07527337	42.48407597	0.29918363	0.59836727	0.10712072
50 g/L NaCl	$y = -6.50314 + 10\ln(x + 0.05957)$	3.09961474	31.98764101	0.22526508	0.45053016	0.04572372
75 g/L NaCl	$y = -2.84106 + 9.47894\ln(x - 0.15982)$	2.44674593	25.08113086	0.17662768	0.35325536	0.02204125
100 g/L NaCl	$y = -1.48123 + 9.14998\ln(x - 0.23662)$	2.2672228	23.1981825	0.16336748	0.32673496	0.01744042
150 g/L NaCl	$y = -2.25513 + 9.87099\ln(x - 0.23692)$	2.32209193	23.77294898	0.16741513	0.33483027	0.01876913
200 g/L NaCl	$y = -0.45 + 9.34\ln(x - 0.32)$	2.11232163	21.57903488	0.15196503	0.30393007	0.01403754

Appendix D: Experimental error of Na₂SO₄ solubility at three NaCl concentrations

Table A11 Error calculation about three concentrations of NaCl under different temperature

Temperature (°C)	Error (%)		
	50 g/L NaCl	100 g/L NaCl	150 g/L NaCl
18	-3.041	7.839	5.301
16.5	-0.077	9.443	4.803
15	2.538	10.722	4.151
13.5	4.803	11.666	3.322
12	6.715	12.270	2.294
10.5	8.271	12.524	1.047
9	9.469	12.419	-0.440
7.5	10.307	11.941	-2.195
6	10.781	11.071	-4.251
4.5	10.889	9.782	-6.646
3	10.632	8.035	-9.430
1.5	10.008	5.782	-12.662
0	9.018	2.957	-16.416
-1.5	7.723	-0.452	-20.704
-3.2	-15.112	-4.602	-25.685
-4.5	-	-9.605	-31.477
-6	-	-15.601	-38.211
-7.5	-	-	-46.044
-9	-	-	-55.165
-9.45	-	-	-58.862

Appendix E: Decreasing rate of the solubility of Na₂SO₄ with temperature at different NaCl/KCl concentrations

Table A12 The decreasing tendency of the solubility of Na₂SO₄ with temperature when NaCl concentration changed

Temperature (°C)	Decreasing percentage (%)			
	0-50 g/L KCl	50-100 g/L KCl	100-150 g/L KCl	150-200 g/L KCl
18	22.556	17.875	10.599	2.556
16.5	24.668	19.428	11.514	3.240
15	26.864	20.908	12.257	3.724
13.5	29.155	22.309	12.838	4.042
12	31.547	23.619	13.264	4.220
10.5	34.039	24.823	13.542	4.278
9	36.631	25.905	13.679	4.233
7.5	39.313	26.849	13.683	4.099
6	42.075	27.642	13.562	3.886
4.5	44.902	28.271	13.325	3.606
3	47.773	28.727	12.980	3.265
1.5	50.670	29.005	12.536	2.871
0	53.570	29.101	12.000	2.429

Table A13 The decreasing tendency of the solubility of Na₂SO₄ with temperature when KCl concentration changed

Temperature (°C)	Decreasing percentage (%)			
	0-50 g/L KCl	50-100 g/L KCl	100-150 g/L KCl	150-200 g/L KCl
18	14.152	10.530	8.091	13.311
16.5	15.241	11.428	8.229	14.587
15	16.404	12.373	8.357	15.983
13.5	17.641	13.349	8.476	17.490
12	18.951	14.339	8.586	19.101
10.5	20.339	15.328	8.690	20.808
9	21.806	16.299	8.786	22.606
7.5	23.361	17.232	8.876	24.487
6	25.007	18.112	8.961	26.445
4.5	26.752	18.918	9.040	28.474
3	28.602	19.636	9.114	30.568
1.5	30.563	18.306	9.197	34.886
0	32.638	19.340	9.257	23.013

Appendix F: Decreasing and decreasing rate of the solubility of Na_2SO_4 with temperature

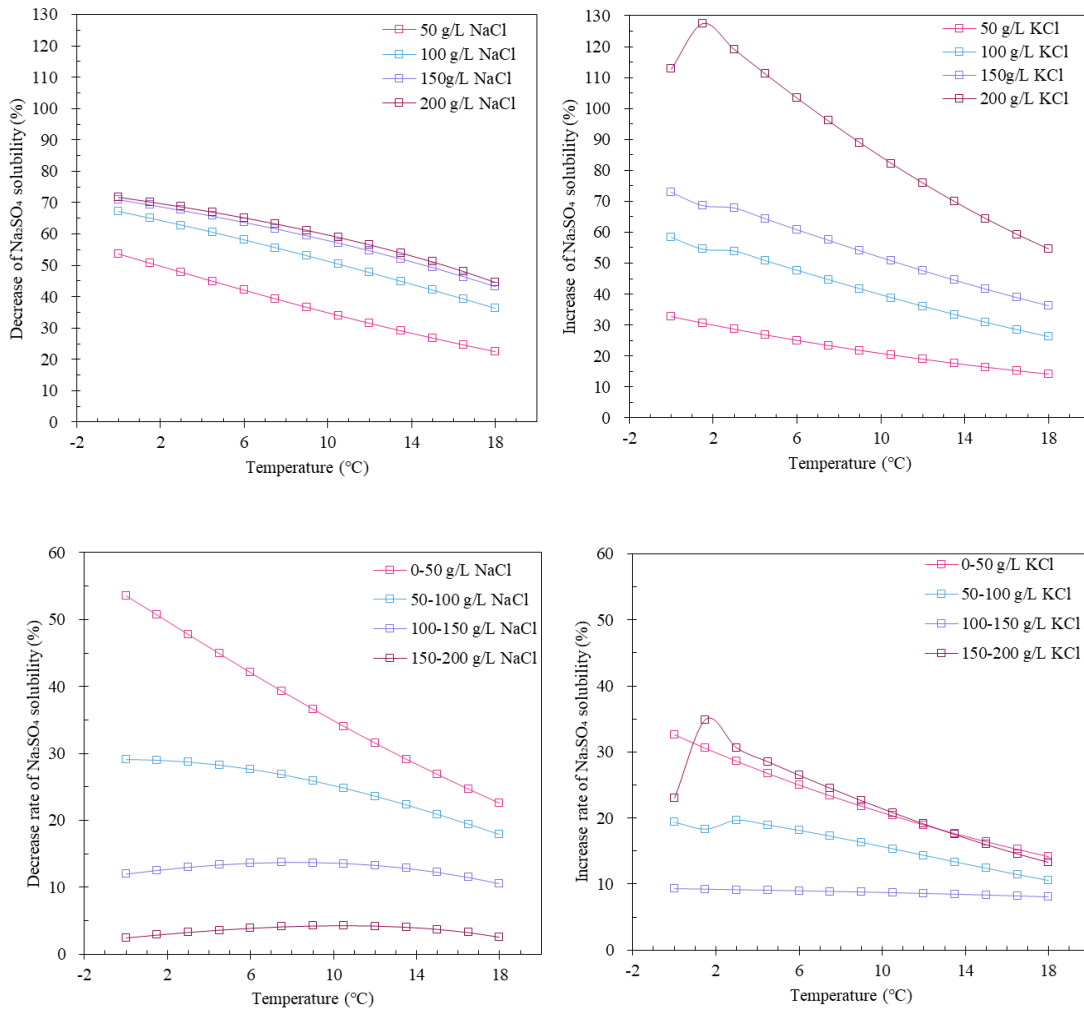


Figure A4 The decreasing and decreasing rate of Na_2SO_4 solubility with temperature at different NaCl(left) or KCl(right) concentrations

(a) Compares the falling percentage in the solubility of Na_2SO_4 with and without NaCl. (b) Compares the rising percentage in the solubility of Na_2SO_4 with and without KCl. (c) At the same temperature, the higher the concentration of NaCl, the less decreasing rate the solubility of Na_2SO_4 . Decreasing the temperature, the higher the concentration of NaCl, the decreasing tendency of Na_2SO_4 solubility with temperature. (d) The effect of KCl was almost the same as NaCl, except at 150-200 g/L that the change of Na_2SO_4 solubility accelerated with decreasing temperature.

Appendix G: Temperature profile of the EFC process

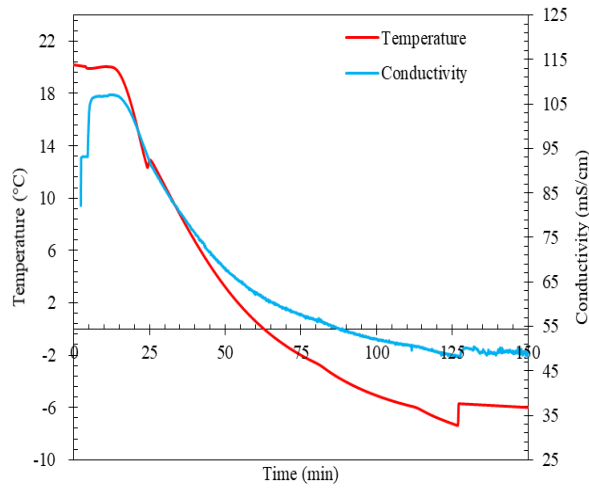


Figure A5 Temperature and conductivity profile during EFC

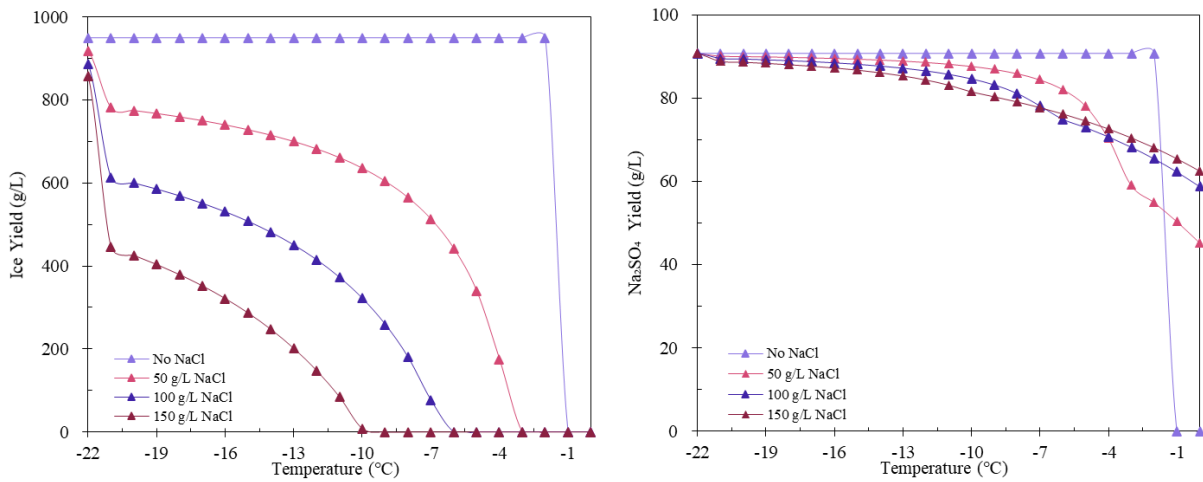


Figure A6 Ice and mirabilite yield during the cooling process under the different NaCl concentrations
 Continuous EFC process with 1 L solution of 40 g/L Na_2SO_4 and NaCl (0-150 g/L)